

AD-A127 229

DEEP LEVEL DEFECTS IN SEMICONDUCTORS(U) ILLINOIS UNIV
AT CHICAGO CIRCLE DEPT OF PHYSICS S SUNDARAM ET AL.

1/1

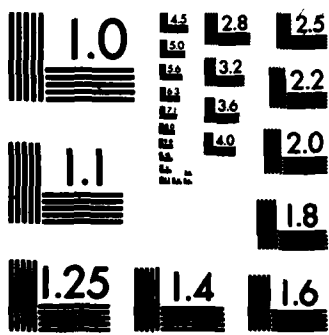
JUL 80 N00014-78-C-0732

UNCLASSIFIED

F/G 20/12

NL





MICROCOPY RESOLUTION TEST CHART
NATIONAL BUREAU OF STANDARDS-1963-A

1-1247
1
AD A127229

Deep Level Defects in Semiconductors

S. Sundaram

R. R. Sharma

Department of Physics

University of Illinois at Chicago Circle
Chicago, Illinois 60680

July 1980

FINAL TECHNICAL REPORT

July 1, 1979 - June 30, 1981

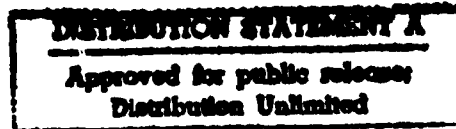


Prepared for

Office of Naval Research
Arlington, Virginia 22217

U.S. ONR Contract No. N00014-78-C0732

DMC FILE COPY



83 04 20 104

DD FORM 1 JAN 73 1473

EDITION OF 1 NOV 65 IS OBSOLETE
S/N 0102-LF-014-6601

SECURITY CLASSIFICATION OF THIS PAGE (When Data Entered)

CONTENTS

	Page
Abstract	1
Introduction	2
Intracenter Transition in InP:Fe and GaAs:Fe	3
Energy Levels of GaAs:Cr ²⁺ and GaAs:Cr ³⁺	10
Theory of g-factors and Charge Transfer in GaAs:Cr ²⁺	15
Interaction Constants for Ions in Crystals	19
Conclusion	23
Acknowledgment	25
References	26

Accession For	
NTIS GRA&I <input checked="" type="checkbox"/>	
DTIC TAB <input type="checkbox"/>	
Unannounced <input type="checkbox"/>	
Justification	
By _____	
Distribution/ _____	
Availability Codes	
Dist	Avail and/or Special



A

Deep Level Defects in Semiconductors

Abstract

Using Racah's irreducible tensor operator formalism, a generalized and more refined treatment of the d-electron matrices for transition metal defects in crystal has been given. The resulting Coulomb and exchange interaction matrices have been used to calculate the electronic structures of GaAs:Cr²⁺ and GaAs:Cr³⁺ and interpret the optical data on MgF₂:Co²⁺ and MgF₂:Mn²⁺. The significance of the new theory is explained. From the photoluminescence and optical absorption data, the crystal field parameters have been derived for GaAs:Fe and InP:Fe. The theory of the charge transfer effects on the electronic structure of GaAs:Cr²⁺ have been discussed and a ligand-field model has been developed for explaining the optical and EPR results of GaAs:Cr²⁺.

1. Introduction

The program described in this final report is part of an over-all program dealing with defect centers in III-V semiconductor materials that are of importance for opto-electronic device applications. Specifically, the investigations relate to the optical studies of transition metal impurities in GaAs and InP giving rise to deep level centers. The report consists of the results on (i) the derivation of the crystal field parameters that will best explain the photoluminescence results of InP:Fe and optical absorption at low temperatures of GaAs:Fe; (ii) the derivation of the generalized d-electron interaction matrices for defect centers in crystals and the calculations of the electronic structures of GaAs:Cr^{2+} and GaAs:Cr^{3+} ; and (iii) the considerations of the charge transfer effects affecting the g-factors and the zero field splitting parameters in GaAs:Cr^{2+} leading to the interpretation of the EPR results of the system. In addition, from the generalized treatment of the electron-electron interaction matrices we have also provided the interpretation of optical data on $\text{MgF}_2:\text{Co}^{2+}$ and $\text{MgF}_2:\text{Mn}^{2+}$. The remaining part of this report consists of four parts (Section 2-5) and supplements our published article,^{1,2} as well as the presentations at the American Physical Society meetings³⁻⁶ and the ones that have been submitted to journals or are under preparation. While this report summarizes the results of our studies thus far, further information on any of the topics discussed in this report may be obtained from the investigators.

2. Intracenter Transitions in InP:Fe and GaAs:Fe

The transition metal impurities associated with compensation and control of electrical properties of semiconductors give rise to deep levels in the forbidden gap. While the nature of the deep level impurities in II-VI semiconductors has been studied extensively by contrast the nature of these impurities in III-V compounds has not received much attention until recently. The positions of the impurity centers, their charge states, and the nature of the recombination processes are all very relevant to the behavior of III-V materials and their uses in device applications.

The present study on the interpretation of the photoluminescence and optical absorption experimental results was undertaken as part of our systematic study of the deep level defect centers in GaAs and InP. The studies on Fe in III-V materials have been limited to GaAs in most studies⁷⁻¹². The only studies of Fe in InP are the recent measurements of Koschel *et al*^{12,13} establishing Fe^{2+} as a possible charge state for the ion. The photoluminescence emission peaks observed in the infrared and their behavior with temperature have been used in our investigation to establish that the mechanism can be explained as arising from intracenter transition. There are four prominent lines observed in the photoluminescence spectrum of InP:Fe. They are at 2801 cm^{-1} , 2819 cm^{-1} , 2830 cm^{-1} , and 2843 cm^{-1} . A comparison of the PL spectrum with the optical absorption indicates that crystal field theory applied to $\text{Fe}^{2+}(3d^6)$ in a tetrahedral (T_d) environment of the host crystal InP can satisfactorily account for the observed lines. Group-theoretical arguments lead to the splitting of the term 5D of the free ion Fe^{2+} into orbital doublet $^5E(\Gamma_3)$ and orbital triplet $^5T_2(\Gamma_5)$ in T_d . Due to the second order spin-orbit interaction effects the orbital doublet will split into five levels and the orbital triplet will give rise to six

levels according to

$$D_2 \times r_3 = r_1 + r_2 + r_3 + r_4 + r_5$$

and

$$D_2 \times r_5 = r_1 + r_2 + r_3 + r_4 + r_5$$

(see scheme in Fig. 1). Due to lower nonequilibrium electron populations of the higher levels of the excited state 5T_2 and the possible rapid thermalization of higher states to the lowest level r_5 of 5T_2 by non-radiative transitions, one need consider only the transitions from the lowest level of 5T_2 to the split levels of 5E . The transition $r_5(T_2) \rightarrow r_2(E)$ is forbidden and this leaves four allowed transitions.

In Table I we have summarized the frequencies observed for InP:Fe²⁺, the assignments, and the expressions for the energy differences in terms of the crystal field parameters ($=10Dq$), λ_1 and λ_2 (the spin-orbit interaction parameters). From the expressions for the energies, the separation between the observed PL peaks should be equal to the theoretical splitting $6\lambda_2^2/\Delta$. Using an average value of 14 cm^{-1} for this separation $6\lambda_2^2/\Delta$ from the experimental data, a value of 84 cm^{-1} is derived for λ_2 corresponding to 300 cm^{-1} for Dq . For the range of 260 to 310 cm^{-1} for Dq , one gets $\lambda_2 = 81 \pm 4 \text{ cm}^{-1}$. The mean values of the crystal field parameters derived in our study are

$$\Delta = 3028 \text{ cm}^{-1} \text{ and } |\lambda_1| = \lambda_2 = 83 \text{ cm}^{-1}.$$

Table II shows the data⁹ on low temperature optical absorption by GaAs:Fe. The assignments of the observed transitions by Ippolitova et al.,⁹ are also shown in Table II. The labels correspond to the numbers given in Fig. 1. On the basis of the assignments, the following crystal field parameters have been obtained by the previous authors.⁹

Fig. 1
Transitions ${}^5T_2 - {}^5E$

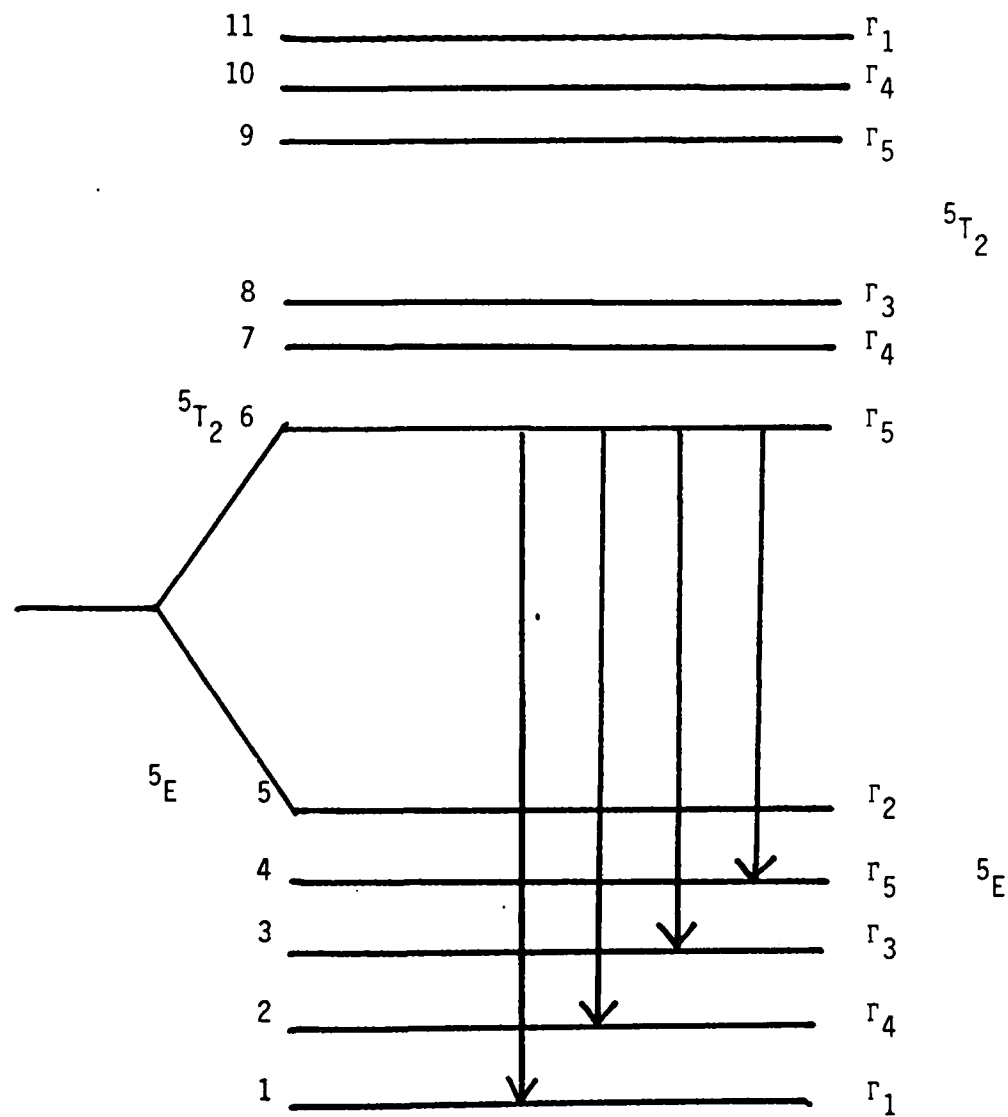


Table I Intracenter Transitions of InP:Fe²⁺

Transition*	Frequency(cm ⁻¹)	Energy
6 - 1	2843	$\Delta + 3\lambda_1 + 138 \lambda_2^2/5\Delta$
6 - 2	2830	$\Delta + 3\lambda_1 + 108 \lambda_2^2/5\Delta$
6 - 3	2819	$\Delta + 3\lambda_1 + 78 \lambda_2^2/5\Delta$
6 - 4	2801	$\Delta + 3\lambda_1 + 48 \lambda_2^2/5\Delta$

* See Fig. 1

Table II Optical Absorptions for GaAs:Fe²⁺

Transition* (Previous Assignment)	Frequency(cm ⁻¹)	Revised Assignment	Energy
1 - 6	3002	1 - 6	$\Delta + 3\lambda_1 + 138 \frac{\lambda_2^2}{5\Delta}$
1 - 9	3092	2 - 8	$\Delta - 2\lambda_1 + \frac{132}{5} \frac{\lambda_2^2}{\Delta}$
2 - 6	2988	2 - 6	$\Delta + 3\lambda_1 + 108 \frac{\lambda_2^2}{5\Delta}$
2 - 7	3044	4 - 8	$\Delta + \lambda_1 + 24 \frac{\lambda_2^2}{\Delta}$
2 - 8			$\Delta + \lambda_1 + \frac{30\lambda_2^2}{\Delta}$
3 - 6	2979	3 - 6	$\Delta + 3\lambda_1 + 78 \frac{\lambda_2^2}{5\Delta}$
4 - 6	2962	4 - 6	$\Delta + 3\lambda_1 + 48 \frac{\lambda_2^2}{5\Delta}$

* See Fig. 1

$$\Delta = 2995 \pm 10 \text{ cm}^{-1}, \lambda_1 = 18 \pm 2 \text{ cm}^{-1}, \lambda_2 = 77 \pm 6 \text{ cm}^{-1}$$

We have made a systematic review of the above optical absorption data and the results for the crystal field parameters obtained by the previous authors.⁹ Though the covalency effects can reduce the free ion values for λ_1 and λ_2 by ~20% as pointed out by Wong¹⁴ it seems highly improbable that a value as low as 18 cm^{-1} can be obtained for λ_1 . There seems to be an error also in the sign of λ_1 . These prompted our review of the assignments⁹ of the observations, particularly those at 3092 cm^{-1} and 3044 cm^{-1} . The assignments of the transitions to 1-9 and 2-7 or 2 respectively do not seem plausible on the basis of the value of λ_1 or separations of the observed transitions. A revised assignment of these two bands to 2-8 and 4-8 transitions seem to be reasonable and these are allowed by selection rules. With these revised assignments, all the observed absorption lines for GaAs:Fe yield the following values:

$$\Delta = 3028 \text{ cm}^{-1}, \lambda_1 = -44 \text{ cm}^{-1} \text{ and } \lambda_2 = 83 \text{ cm}^{-1}.$$

We have compared the values for InP:Fe and GaAs:Fe in Table III, and there is a close agreement between the two sets of values and the values obtained by Bykovski *et al.*,¹⁰ who report a value of -90 cm^{-1} for λ_1 . Thus in summary, the photoluminescence data on InP:Fe and the low temperature optical absorption data on GaAs:Fe have been interpreted as arising from intracenter transitions and the crystal field parameters of Δ , λ_1 , and λ_2 have been derived from the above data. The revised assignments for GaAs:Fe provided by our study give better sets of values as may be seen from Table III and by comparison with results on II-VI materials.

Table III Crystal Field Parameters in cm^{-1} for InP:Fe²⁺ and GaAs:Fe²⁺

System	$\Delta = 10 \text{ Dq}$	λ_1	λ_2
InP:Fe ²⁺	3028	-83	83
GaAs:Fe ²⁺	3028 (2995)*	-44 (-18)*	82 (77)*

* Values in Parentheses are from Ref. 9.

3. Energy Levels of GaAs:Cr²⁺ and GaAs:Cr³⁺

In this section we present a major advance for the first time in the theoretical treatment of the d-electron interactions in order to facilitate the theoretical understanding of the experimental observations on the III-V materials of GaAs and InP containing transition metal impurities as defect centers. It is well known that up to now most of the theoretical treatments have been restricted to the use of the "pure" d-orbitals in calculating the electron-electron interactions in complexes and solids. In our attempts to investigate systematically the nature of defect centers in GaAs and InP we have encountered the difficulties associated with the unavailability of the explicit generalized form of Tanabe-Sugano matrix elements¹⁵ for the single particle electronic wavefunctions which are not of the "pure" d-character. The theory that was widely adopted for interpreting the optical spectra of transition metal ions in solids and complexes is the one by Racah¹⁶ using only three parameters B, C, and A. As is well known, despite the useful simplifications this theory provided, it suffers from serious drawbacks in neglecting the important solid state effects such as the modifications of the wavefunctions from the pure d character. There are a number of examples in which it has been shown that this simple theory is glaringly inadequate. Therefore, it is extremely important to improve the theory and we have adopted the strong field coupling scheme^{15,17} (since many physical cases of interest come under this category), to provide the refinement to d-electron interactions.

In our treatment, which also adopts Racah's irreducible tensor operator formalism, we have derived the generalized electron-electron interaction matrices in terms of ten independent Coulomb and Exchange parameters V_1, V_2, \dots, V_{10} (or a, b, c, ..., j) defined in the standard Dirac notation and the one-electron orbitals $\psi_1, \psi_2, \psi_3, \psi_4$, and ψ_5 in the cubic-field representations.

The matrix elements for d^2 , d^3 , d^4 , and d^5 configurations in octahedral symmetry are tabulated in the attached reprint (Ref. 2). As might be inferred, if σ , ϵ , t , e , n , λ are reduced to pure d-type orbitals, these matrix elements reduce to the forms given by Tanabe and Sugano.¹⁵ In addition, using group-theoretical methods the matrix elements of the complementary states d^{10-n} ($n = 2, 3, 4, 5$) have been derived by us. Of particular significance in the general expression that we have derived connecting the complementary states in the form

$$\begin{aligned} & \langle t_2^{6-m}(s_1r_1)e^{4-\lambda} | s_2r_2 | S^m M_\Gamma | (e^2/r_{12}) | t_2^{6-n}(s_1r_1) \\ & e^{4-\lambda}(s_2r_2) S^m M_\Gamma \rangle - \langle t_2^m(s_1r_1)e^\lambda | s_2r_2 | \\ & S^m M_\Gamma | (e^2/r_{12}) | t_2^m(s_1r_1)e^\lambda | s_2r_2 | S^m M_\Gamma \rangle \\ & = (3-m)V_1 + 4(3-m)V_2 + \frac{(24-4m-6\lambda)}{\sqrt{3}}(V_3 + V_4) + \frac{(6-3\lambda)}{\sqrt{3}}V_5 \\ & + (5\lambda-10)V_6 + (2m+3\lambda-12)V_7 + (2m+3\lambda-12)V_8/\sqrt{3} - 2(3-m)V_{10} \end{aligned}$$

where the integers m and λ are connected to n (in d^n configuration) by the relation

$$m + \lambda = n \quad \text{or} \quad 10-n.$$

Equally significant is the fact that we have shown that the diagonal matrix elements of d^{10-n} states differ from the corresponding elements of d^n by different amounts that are linear combinations of V_i 's. This is in contrast to the constant differences resulting in the case of pure d-orbitals.

The matrix elements derived in the present study for d^3 and d^4 configurations were used to obtain the energies for GaAs:Cr³⁺ and GaAs:Cr²⁺. Recently, Hemstreet and Dimmock¹⁸ have calculated the above electronic structure by modifying the e and t_2 symmetry orbitals using parameters R_{ee} ,

R_{tt} , R_{et} deduced from X_1 calculations. We have calculated the energies of GaAs:Cr²⁺ and GaAs:Cr³⁺ using our generalized matrix elements and these results are presented in Figures 2 and 3. Except for some minor differences that we have pointed out in our publication², there is general agreement between our results and those of the earlier study.¹⁸

While our new theory has more parameters (eleven of them V_1 , V_2 ... V_{10} , Δ) instead of four parameters (A , B , C , Δ) or more precisely only three parameters (B , C , Δ) used by Racah¹⁶, the full significance of our theory lies in the potential application to a variety of physical problems in the correct way and the generality of our superior formalism. This is further clarified in Part 5 of this report involving refined interpretation of the spectra of other systems and the evaluation of Coulomb and Exchange interaction constants.

Fig. 2

Energy Levels for GaAs:Cr²⁺

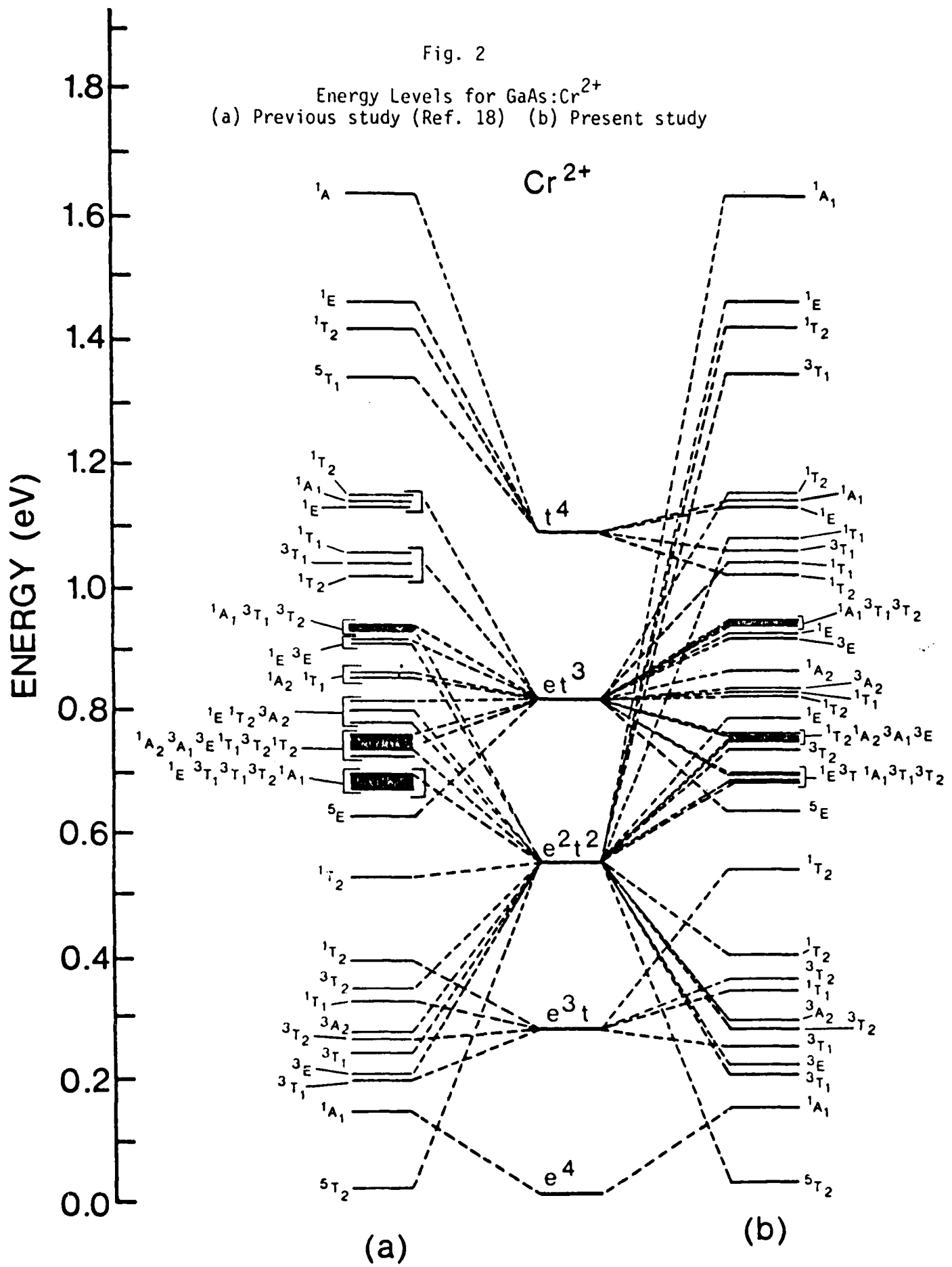
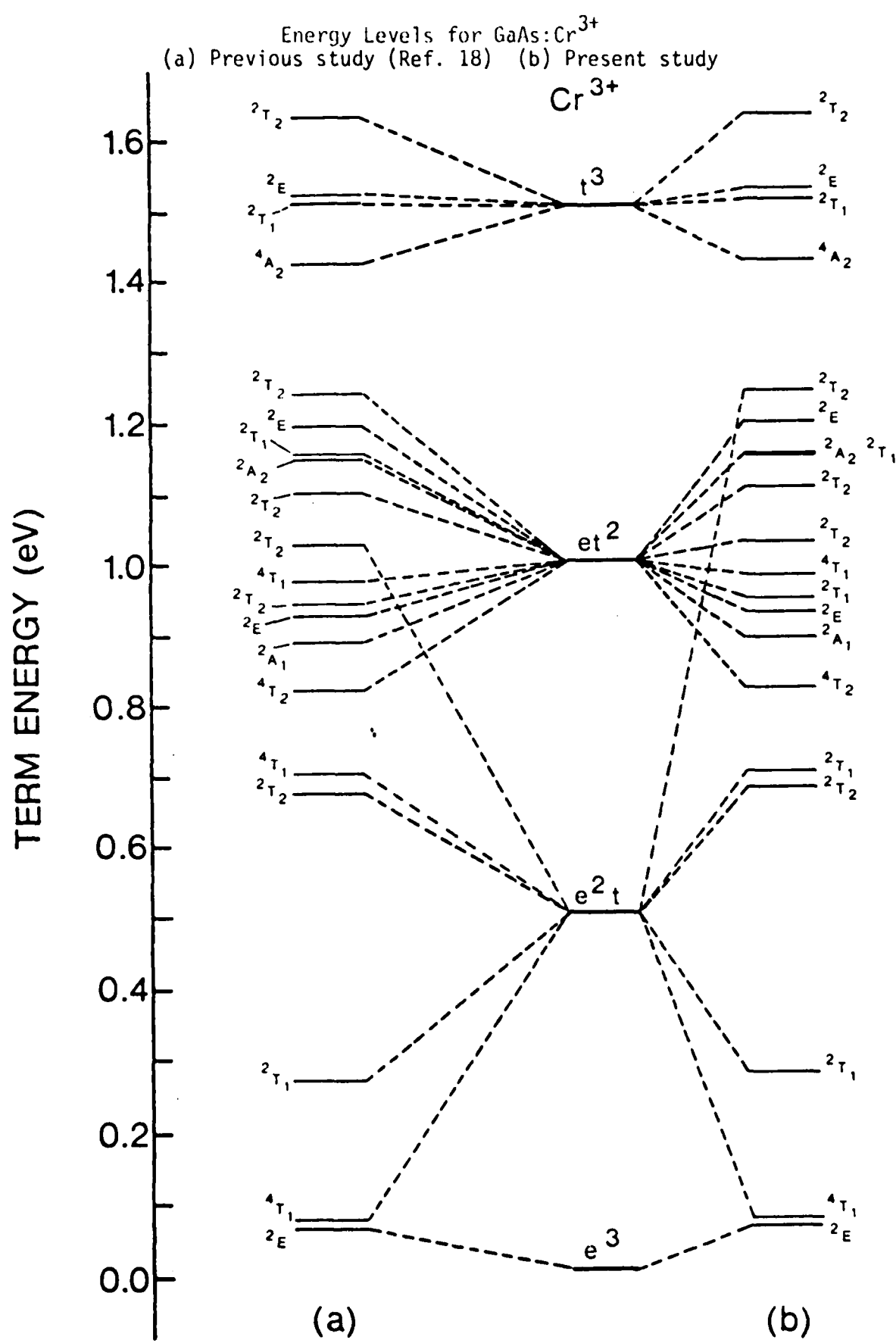


Fig. 3



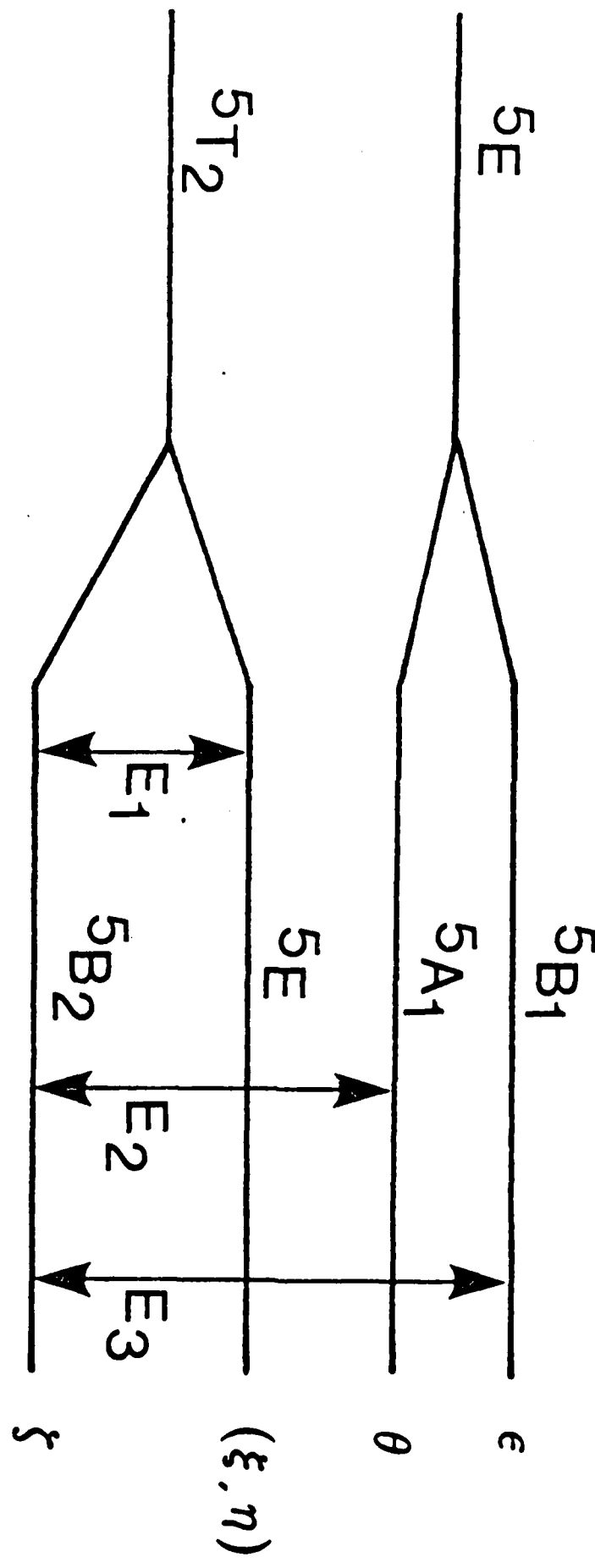
4. Theory of g-factors and Charge Transfer in GaAs:Cr²⁺

As part of our continuing studies of transition metal impurity defect centers in GaAs, in this section we present the results of some of our preliminary investigations on the nature of Cr²⁺ center in GaAs and the interpretation of EPR experimental data. Although GaAs:Cr²⁺ has been the subject of several theoretical and experimental studies particularly with respect to the electronic structure of the ground state of the impurity, many theoretical questions for the excited states of the impurity ion still remain unanswered. Electron paramagnetic resonance (EPR)¹⁹ and ultrasonic attenuation²⁰ experiments have established that GaAs:Cr²⁺ undergoes a Jahn-Teller distortion resulting in a change from tetrahedral (T_d) to tetragonal (D_{2d}) symmetry at the Cr²⁺ site. The upper state 5E of the 0.84 eV transition ($^5E \rightarrow ^5T_2$) observed in photoluminescence experiments²¹ splits into 5A_1 and 5B_1 states of D_{2d} symmetry while the ground state 5T_2 splits into 5B_2 and 5E states in the tetragonal symmetry as a result of Jahn-Teller (JT) distortion. (See Fig. 4) Such results are also consistent with photconductivity measurements.^{22,23} In a similar study on analogous II-VI materials with Cr²⁺, Vallin and Watkins²⁴ approached the problem through a molecular orbital treatment. Though they used only one parameter, the study did reveal the importance of the charge transfer effects on the magnetic properties of the impurities in such systems.

In view of the presence of Jahn-Teller distortion and the importance of charge transfer effects we have studied as part of this project the molecular cluster Cr²⁺-As₄. The present molecular orbital treatment in the framework of the ligand-field theory involves the construction of molecular orbitals using the d-orbitals of Cr²⁺ and the outermost s and p-orbitals of the As atoms. In terms of the cubic field representation 0, e, ξ , n, λ ,

Fig. 4

Splitting due to Jahn-Teller distortion ($T_d \rightarrow D_{2d}$)



cluster wavefunctions ψ_{\parallel} , ψ_{\perp} belonging to 5E and $\psi_{\perp}, \psi_{\parallel}, \psi_{\perp}$ belonging to 5T_2 and were constructed and the expressions for g_{\parallel} , g_{\perp} , and D in the spin-Hamiltonian were derived in our study. The details of such calculations and the exact forms of the expressions for wavefunctions involving the admixture parameters will be given in an article to be published. The EPR results obtained by Krebs and Stauss¹⁹ give $g_{\parallel} = 1.974$, $g_{\perp} = 1.997$, and $D = -1.860 \text{ cm}^{-1}$. In our study we have obtained the spin-orbit matrix elements $\zeta_{d,d} (\text{Cr}^{2+})$ and $\zeta_{p,p} (\text{As})$ as 303 cm^{-1} and 1246 cm^{-1} respectively. These values lie close to the corresponding values of 236 cm^{-1} and 1273 cm^{-1} given by Abragam and Bleaney²⁵. In the present investigation, the overlap and two-center integrals were calculated and the values of admixture parameters (λ 's) that will best explain the EPR results (g_{\parallel} , g_{\perp} , and D) were derived. These values are

$$\lambda_{dp_{\parallel}} = 0.491$$

$$\lambda_{ds} = 0.281$$

$$\lambda_{dp_{\perp}} = 0.110.$$

Assuming the λ 's are sums of the corresponding overlap and charge transfer covalency parameters, the values of the charge transfer covalencies obtained in the present study are

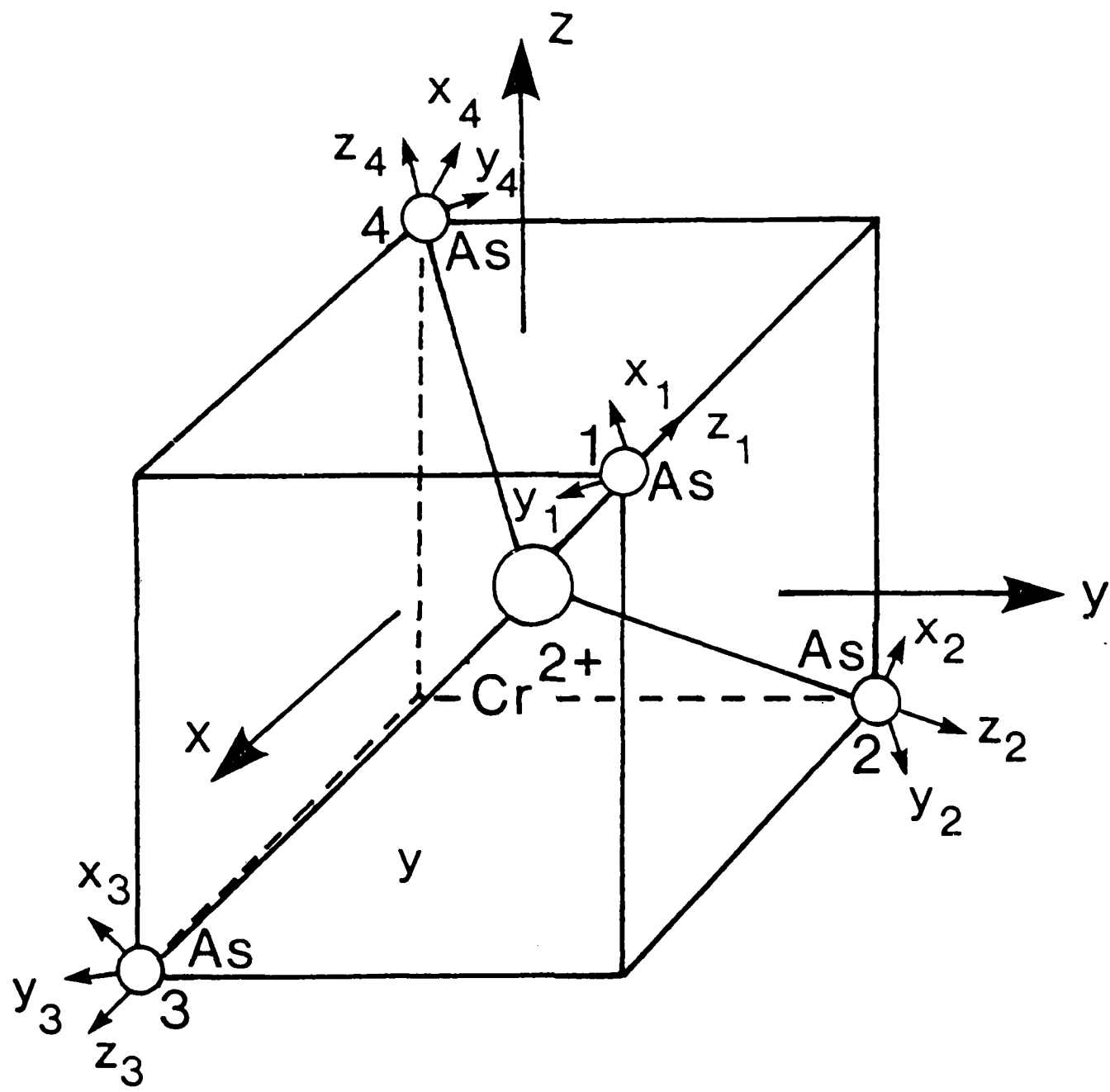
$$r_{dp_{\sigma}} = 0.583$$

$$r_{ds} = 0.214$$

$$r_{dp_{\pi}} = 0.049.$$

These values are significant and reveal the nature of the defect center Cr^{2+} in GaAs and can also be used to derive more accurate Coulomb and exchange matrix elements. The cluster $\text{Cr}^{2+} - \text{As}_4$ is shown in Fig. 5.

Fig. 5
Molecular cluster $\text{Cr}^{2+}\text{-As}_4$



5. Interaction Constants For Ions In Crystals

As was mentioned earlier, one of our main goals was to provide a refined treatment for the interaction matrices for transition metal ions in crystals. In the process of deriving a new formalism and providing the generalized matrices we have come across the detailed optical spectra of systems involving transition metal ions Co^{2+} and Mn^{2+} in MgF_2 system. Though the system is not of direct interest to our series it was felt that the new theory should be verified by application to a system where there are abundant lines observed experimentally. The experiments²⁶ on the above mentioned system have made available many sharp lines of the transition metal ions in crystals by lifting the spin-forbidden characteristics of the excitations through exchange interactions with color centers. The refined formalism that we have derived was applied in the present investigation to analyze the spectra of $\text{MgF}_2:\text{Co}^{2+}$ and $\text{MgF}_2:\text{Mn}^{2+}$.

In this section of the report we have shown (i) the application of the new formalism enables for the first time the direct calculation of Coulomb and Exchange crystal field parameters and (ii) the refined theory gives a proper interpretation of the detailed optical spectra unlike the simple three-parameter B , C , Δ theory. As may be seen from our published work¹, the application of the new formalism to evaluate the Coulomb and exchange interaction constants would require solving the inverse-eigenvalue problem using the observed optical spectra. The observed lines for $\text{MgF}_2:\text{Co}^{2+}$ from the data of Sibley et al²⁶ were used along with our matrix elements and the general formula derived in our present study relating the diagonal elements of complementary configurations.

In solving the inverse eigenvalue problem and obtain V_i 's ($i = 1$ to 10)

it is necessary to have a sufficient number of lines from optical spectra. For $MgF_2:Co^{2+}$, eleven well defined lines were available and ten of these were used in the inverse eigenvalue problem and the remaining one was used to check the validity of the solution. To our knowledge there are no calculated values of Coulomb and exchange interaction constants in the systems we have investigated. Table IV gives the Coulomb and exchange crystal field parameters and a comparison with the corresponding values for the free ion calculated by us using the wavefunctions given by Clementi (see Ref. 1). Also, we have shown in Table V the comparison of the observed and calculated energy values together with previous tentative assignments²⁶ and the revised assignments. It is very significant that our analysis has provided the correct assignments to many of the lines as shown in Table V.

The application of the inverse eigenvalue problem to the data on $MgF_2:Mn^{2+}$ with our matrix elements for d^5 configuration resulted in a matrix of dimension 43x43 compared to 20x20 for Co^{2+} . The values of the parameters for Mn^{2+} case are also given in Table IV. Again we have compared them with corresponding free ion values calculated by using Clementi's wavefunctions. As was pointed out earlier there are no previous values for V_i 's from other sources for comparison. We have thus shown for the first time it is possible to obtain them using our refined formalism. Also, we have determined that many of the tentative assignments of the lines belonging to this system have to be revised (see also our paper Ref. 1).

Table IV Coulomb and Exchange Interaction Constants in Cm^{-1}

System	$v_1 - v_2$	$v_1 - v_4$	$v_1 - v_5$	v_3	v_6	v_7	v_8	v_9	v_{10}	10	Dq
$\text{MgF}_2:\text{Co}^{2+}$	13034	13728	-2433	2725	8491	3219	1928	1259	6257	-7250	
Free Ion*	16920	16920	0	4379	9724	5932	2189	2189	8460	—	
$\text{MgF}_2:\text{Mn}^{2+}$	11176	11931	647	2469	6026	2725	1584	2164	6093	5710	
Free Ion*	15328	15328	0	3958	8806	5378	1979	1979	7664	—	

* Values calculated using Clementi's wavefunctions.

Table V Observed and Calculated Energy Values in cm^{-1} for $\text{MgF}_2:\text{Co}^{2+}$

Previous Assignment*	Present Assignment	Observed Energy Value	Calculated Energy Value
$^4\text{T}_{2g} ({}^4\text{F})$	$^4\text{T}_{2g} ({}^4\text{F})$	7519	7518.9
$^2\text{E}_g ({}^2\text{G})$	$^2\text{E}_g ({}^2\text{G})$	11905	11904.9
$^4\text{A}_{2g} ({}^4\text{F})$	$^4\text{A}_{2g} ({}^4\text{F})$	15385	12205.1
$^2\text{T}_{1g} ({}^2\text{G})$	$^2\text{T}_{2g} ({}^2\text{G})$	17452	17452.1
$^4\text{T}_{1g} ({}^4\text{P})$	$^4\text{T}_{1g} ({}^4\text{P})$	$\left. \begin{array}{l} 18519 \\ 19305 \\ 20921 \end{array} \right\}$	19305
$^2\text{A}_{1g} ({}^2\text{G})$	$^2\text{T}_{1g} ({}^2\text{G})$	20833	20832.9
$^2\text{T}_{1g} ({}^2\text{H})$	$^2\text{A}_{1g} ({}^2\text{G})$	21739	21739
$^2\text{T}_{2g}, {}^2\text{T}_{1g} ({}^2\text{H})$	$^2\text{T}_{2g} ({}^2\text{H})$	$\left. \begin{array}{l} 23095 \\ 23529 \end{array} \right\}$	23094.9
$^2\text{E}_g ({}^2\text{H})$	$^2\text{E}_g ({}^2\text{H})$	25000	23529
			26968.9

* Ref. 26.

6. Conclusion

(1) In this program we have examined in detail the photoluminescence data on InP:Fe and the low temperature optical absorption results on GaAs:Fe and derived the set of crystal field parameters that will best describe the experimental observations. The results can be explained as intracenter transitions.

(2) For the d^n configurations of defect centers we have proposed a new refinement for the theory of electron-electron interactions and derived the generalized d-electron matrices for d^n ($n = 2, 3, 4, 5$). Further, we have derived the significant relation connecting the complementary configurations d^n and d^{10-n} and shown that in the generalized case the diagonal elements of the matrices do differ by varying amounts. We have applied our generalized theory to GaAs:Cr²⁺ and GaAs:Cr³⁺ cases and obtained energies in good agreement with previous work by Hemstreet and Dimmock who proposed modifications of e and t_2 orbitals using parameters from X_c calculations.

(3) As part of the defect center problem, we have examined the effect of Jahn-Teller distortion and presented a molecular orbital treatment in the framework of the ligand-field theory for the cluster Cr²⁺-As₄ in GaAs:Cr²⁺. The charge transfer effects have been derived and the parameters that will interpret the EPR results of Krebs and Stauss have been obtained. These results are significant for accurate calculations of Coulomb and exchange interactions. The effects of charge transfer are shown to be very important.

(4) We have also verified the use of the revised formalism for d-electrons to two other systems (MgF₂:Co²⁺, MgF₂:Mn²⁺) and derived for the first time the complete sets of crystal field parameters. Also, we showed the advantage of the refined treatment to interpret correctly and in detail the observed

optical spectra.

The program has thus established the need for use of generalized d-orbitals and the effects of overlap and charge transfer in elucidating the exact nature of the defect centers in the semiconducting materials GaAs and InP.

Acknowledgment

The support for this research by the contract No. N00014-78-C0732 from the U.S. Office of Naval Research is gratefully acknowledged. The authors also thank Dr. Hemstreet (NRL), Dr. Dimmock (ONR), and Dr. Krebs (NRL) for helpful discussions.

References

1. R.R. Sharma and S. Sundaram, Sol. St. Comm. 33, 381 (1980).
2. R.R. Sharma, M.H. Viccaro, and S. Sundaram, Phys. Rev. B. 23, 738 (1981).
3. R.R. Sharma and S. Sundaram, Bull. Am. Phys. Soc. 24, 255 (1979).
4. M.H. Viccaro, R.R. Sharma, and S. Sundaram, Bull. Am. Phys. Soc. 25, 10 (1980).
5. M.H. Viccaro, S. Sundaram and R.R. Sharma, Bull. Am. Phys. Soc. 25, 326 (1980).
6. M.H. Viccaro, S. Sundaram and R.R. Sharma, Bull. Am. Phys. Soc. 26, 285 (1981).
7. E.M. Ganapolskii, Sov. Phys. Sol. State 15, 269 (1973).
8. Y.N. Fistul, Sov. Phys. Semicond. 8, 311 (1974).
9. G.K. Ippolitova and E.M. Omelyanovskii, Sov. Phys. Semicond. 9, 156 (1975).
10. V.A. Bykovskii et al., Sov. Phys. Semicond. 9, 1204 (1975).
11. E.M. Ganapolskii, Sov. Phys. Semicond. 7, 1099 (1974).
12. W. H. Koschel, et al., Proc. Intl. Conf. Phys. Semicond. Rome (1976).
13. W. H. Koschel, et al., Sol. St. Com. 12, 1069 (1977).
14. J.Y. Wong, Phys. Rev. 168, 337 (1968).
15. Y. Tanabe and S. Sugano, J. Phys. Soc. Japan 9, 753 (1954); 9, 766 (1954).
16. G. Racah, Phys. Rev. 62, 438 (1942); 63, 367 (1942); 76, 1352 (1949).
17. J.S. Griffith, The Theory of Transition-Metal Ions, (Cambridge University Press, N.Y. 1961).
18. L. Hemstreet and J. Dinmock, Phys. Rev. B 20, 1527 (1979).
19. J.J. Krebs and G.H. Stauss, Phys. Rev. B 16, 971 (1977); 20, 795 (1979).
20. H. Tokeemoto and T. Ishiguro, Inst. Phys. Conf. Ser. No. 43, Ch. 9 (1979).
21. W. H. Koschel, S. G. Bishop, and B.D. McCombe, Sol. St. Comm. 19, 521 (1976).

22. U. Kaufmann and J. Schneider, Sol. St. Com. 20, 143 (1976).
23. D.C. Look, Sol. St. Comm. 24, 825 (1977).
24. J.T. Vallin and G.D. Watkins, Phys. Rev. B. 9, 2051 (1974).
25. A. Abragam and B. Bleaney, Electron Paramagnetic Resonance of Transition Metal Ions, Clarendon Press, Oxford (1970).
26. S.I. Yun, L.A. Kappers and W.A. Sibley, Phys. Rev. B 8, 773 (1973).

Generalized *d*-electron interaction matrices—their derivation and impact on existing results

R. R. Sharma, M. H. de A. Viccaro, and S. Sundaram

Department of Physics, University of Illinois, Chicago, Illinois 60680

(Received 2 January 1980)

The restriction of the "pure" *d* orbitals on the Tanabe-Sugano electron-electron interaction matrices has been removed and new matrices have been derived appropriate to *d*-electron transition-metal ions in solids and complexes. We have adopted the group-theoretical technique developed by Racah involving the coefficients of fractional parentage. A general expression useful for obtaining the matrix elements for the complementary states has also been given. The significance of the present study has been emphasized by checking and comparing our results with the recently published results on GaAs:Cr²⁺ and GaAs:Cr³⁺ and by presenting the examples of MgF₂:Co²⁺ and MgF₂:Mn²⁺ where it has been possible to deduce the values of the *d*-electron Coulomb and exchange parameters in conjunction with the fine experimental optical spectra. Other applications such as the removal of accidental degeneracies have been indicated. Important points for further improvements have been discussed.

I. INTRODUCTION

There has been a considerably increasing interest in the study of the transition-metal ions in complexes and solids. The present study is part of our systematic investigations on the defect centers of transition-metal ions in III-V semiconductors of GaAs and InP. Quite recently Hemstreet and Dimmock¹ have calculated many electron-crystal-field term states (besides spin-polarized spin states) for Cr²⁺ and Cr³⁺ in GaAs using an improved approach that is a modification of the standard electron-electron interaction matrix elements^{2,3} by introducing parameters accounting for the changes in the single-particle electronic states in the system. The parameters were deduced from the X-ray scattered-wave cluster calculations which, taken alone, could not account for the electronic structure of Cr in GaAs. In the process of our investigations of the electronic structures of Co²⁺ and Mn²⁺ in solids,⁴ and in our attempts to compare our results for Cr in GaAs with those of Ref. 1, we have encountered the difficulties associated with the unavailability of the explicit generalized form of the Tanabe-Sugano matrix elements for the single-particle electronic wave functions which are not of the "pure" *d* character.

While Hemstreet and Dimmock have suggested the modified approach of removing the restriction of pure *d* nature of the electronic wave functions by introducing three parameters (R_{ee} , R_{et} , and R_{tt}), the advantages of a generalized approach have prompted us to derive the explicit relations and provide a general formalism. We therefore present in this paper the explicit and general forms of the Tanabe-Sugano matrix elements with the aim of making them easily available to the future research workers. We have also used them here to check and compare our results with the calcula-

tions of Hemstreet and Dimmock¹ for Cr²⁺ and Cr³⁺ in GaAs. As will be shown in Sec. III, there is a substantially good agreement between their results (Ref. 1) and those obtained from our present generalized approach. The general matrix elements are also useful for making refined calculations of the transition-metal ions in solids. Recently we have utilized them for designating correctly the energy levels and for deducing the Coulomb and exchange parameters⁴ as well as the refined values of the cubic-field splitting parameter associated with Co²⁺ and Mn²⁺ ions in MgF₂. Moreover, the general treatment is helpful for removing the accidental degeneracy⁵ observed in certain areas.

In Sec. II we give the derived general results with only a brief outline of the method since the method is already well known.^{2,3,6} Section III presents examples which emphasize the effects of the general expressions on the existing results in the literature to justify the importance of our derivations. Section IV deals with the discussion and conclusion.

II. BRIEF OUTLINE OF THE THEORY AND DERIVATION OF MATRIX ELEMENTS

The lack of knowledge of the correct wave functions for the transition-metal ions in a complex or a solid has been a stumbling block to real progress in the theoretical understanding of the experimental observations. Finkelstein and Van Vleck⁷ were the first ones who treated the complex ions in crystals by perturbing the free-ion energy levels due to the crystal environment. Later studies by many authors^{2,3,5,8-11} have helped further our knowledge in this field.

Racah⁸ developed a theory using coefficient of fractional parentage to explain the spectra of free ions and introduced three basic electron Coulomb repulsion parameters *A*, *B*, and *C* for the pure *d*

electrons. This theory was extended to the case of transition-metal ions in solids and complexes by incorporating the effect of the crystal field in terms of the splitting parameter Δ with the assumption that the *d* electrons retain their pure *d* character. This theory has been widely adopted for interpreting the optical spectra of transition metal ions in solids and complexes. In fact, the theory considers only three parameters, B , C , and Δ , as the parameter A plays no role in accounting for the energy differences. While this theory brings forth useful simplifications, it suffers from the serious drawbacks of neglecting the important solid-state effects, such as the modifications of the electron wave functions from the pure *d* character. The faults of the theory are even more noticeable when one recognizes that it really does not work well in many cases.^{5,12,13} For example, a poor agreement has been found by Stevens¹² in the case of Co complexes. Also, the experimental observations¹³ of the optical absorption of Mn^{2+} complex reveals a fine structure, consisting of two peaks separated by 300 cm^{-1} , which cannot be accounted for by considering spin-orbit interaction or departures from cubic symmetry. This splitting, however, can be easily explained on the basis of the present improved theory in which the outer electrons are not restricted to possess the pure *d* character. In that circumstance, the accidental degeneracy in $^4A_{1g}$ and 4E_g predicted by the B , C , Δ theory is innately removed. The mechanism suggested by Koide and Pryce¹⁴ in terms of the mixing of the odd lattice vibrations to explain the $^4A_{1g}$ - 4E_g splitting in Mn^{2+} complexes is really an additional effect besides the one mentioned above.

Thus it is imperative to improve the theory by removing the restriction of the pure *d* nature from the electronic wave functions. To this end, we conceive of the one-electron orbitals as sets of orbitals which form bases for irreducible representations of the symmetry group of the crystal potential. We shall follow the well-known strong-

TABLE I. List of independent Coulomb and exchange integrals.

V_i	Alternate notations	Integral
V_1	a	$\langle \xi\xi e^2 / r_{12} \xi\xi \rangle$
V_2	b	$\langle \xi\eta e^2 / r_{12} \xi\eta \rangle$
V_3	c	$\langle \theta\xi e^2 / r_{12} \epsilon\xi \rangle$
V_4	d	$\langle \epsilon\xi e^2 / r_{12} \epsilon\xi \rangle$
V_5	e	$\langle \theta\theta e^2 / r_{12} \theta\theta \rangle$
V_6	f	$\langle \theta\theta e^2 / r_{12} \epsilon\epsilon \rangle$
V_7	g	$\langle \theta\theta e^2 / r_{12} \eta\eta \rangle$
V_8	h	$\langle \theta\epsilon e^2 / r_{12} \eta\eta \rangle$
V_9	i	$\langle \theta\eta e^2 / r_{12} \xi\xi \rangle$
V_{10}	j	$\langle \xi\xi e^2 / r_{12} \eta\eta \rangle$

field coupling scheme^{2,3} since many physical cases of interest fall in this category. In this scheme, Tanabe and Sugano² have derived the *d*-electron interaction matrices in the simplified picture of pure *d* electrons by utilizing Racah's irreducible tensor operator formalism appropriate to octahedral symmetry. We have adopted the same formalism and have derived the improved matrix elements in terms of the ten independent Coulomb and exchange parameters (Ref. 3) $V_1, V_2, V_3, \dots, V_{10}$ which have been tabulated in Table I in standard Dirac notation for easy reference. The V_i 's are the two-electron matrix elements of the interaction operator e^2/r_{12} between two electrons separated by the distance r_{12} . The functions θ , ϵ , ξ , η , and ζ have been used to denote one-electron orbitals in the cubic-field representation. Evidently these orbitals are no longer of the pure *d* character.

The method of derivation of the electron-electron interaction matrices is well known³ and straightforward but very tedious and time consuming. It is not planned to give details here because it has been described in many places. The electron-electron matrix elements for d^n electrons (with $n = 2, 3, 4$, and 5) derived in the present study are listed in Table II-V for octahedral symmetry. It should be

TABLE II. Tabulation of the electron-electron matrix elements for d^2 electrons in terms of the Coulomb and exchange integrals V_i 's (a, b, \dots , etc.). Asterisk denotes the change in sign with respect to Tanabe-Sugano matrix elements because of the phase conventions.

$^1A_1(d^2)$	$e^2(^1A_1)$	$t_2^2(^1A_1)$
$e^2(^1A_1)$	$e+f$	$\sqrt{6}g+\sqrt{2}h$
$t_2^2(^1A_1)$	$\sqrt{6}g+\sqrt{2}h$	$a+2j$
$^1E(d^2)$	$e^2(^1E)$	$t_2^2(^1E)$
$e^2(^1E)$	$e-f$	$2h^*$
$t_2^2(^1E)$	$2h^*$	$a-j$
$^1T_2(d^2)$	$t_2^2(^1T_2)$	$t_2(t^2T_2)e(^2E)$
$t_2^2(^1T_2)$	$b+j$	$-2i^*$
$t_2(t^2T_2)e(^2E)$	$-2i^*$	$d+g+\sqrt{3}h$ $-c/\sqrt{3}$
$^3T_1(d^2)$	$t_2^2(^3T_1)$	t_{2e}
$t_2^2(^3T_1)$	$b-j$	$-2\sqrt{3}i^*$
t_{2e}	$-2\sqrt{3}i^*$	$d-g+\sqrt{3}c+h/\sqrt{3}$
$^3A_2(e^2) = e - 3f$		
$^3T_2(et_2) = d - g - (1/\sqrt{3})c - \sqrt{3}h$		
$^1T_1(et_2) = d + g + \sqrt{3}c - (1/\sqrt{3})h$		

noted that we have followed the phase conventions of Griffith³ in our derivations. As expected, our matrix elements reduce to the Tanabe-Sugano matrix elements² in case one takes the limiting condition that the θ , ϵ , ξ , η , and ζ orbitals are pure d -

type orbitals. Those matrix elements in Tables II-V which differ in sign on reduction to pure d -orbital case from the corresponding matrix elements obtained by Tanabe and Sugano² (or by Griffith³) have been marked (in the tables) by an asterisk.

TABLE III. Electron-electron matrix elements for d^3 electrons. Asterisk denotes the change in sign with respect to Griffith's matrix elements.

t_2^3	$t_2^3(2E)e^0(^1A_1)$	$t_2^2(^1A_1)e^1(^2E)$	$t_2^2(^1E)e^1(^2E)$	$t^0(^1A_1)e^3(^2E)$	
$t_2^3(2E)e^0(^1A_1)$	$3b$	$-2\sqrt{6}i$	$-\sqrt{6}f^*$	0	
$t_2^3(^1A_1)e^1(^2E)$	$-2\sqrt{6}i$	$a + (2/\sqrt{3})c + 2d$ $-g - (1/\sqrt{3})h + 2j$	$(4/\sqrt{3})c + (2/\sqrt{3})h^*$	$\sqrt{3}g + h$	
$t_2^3(^1E)e^1(^2E)$	$-\sqrt{6}i^*$	$4c/\sqrt{3} + (2/\sqrt{3})h^*$	$a + (2/\sqrt{3})c + 2d$ $-g - (1/\sqrt{3})h - j$	$2h^*$	
$t^0(^1A_1)e^3(^2E)$	0	$\sqrt{3}g + h$	$2h^*$	$3e - 5f$	
t_2^3	$t_2^3(3T_1)e$	$t_2^2(^3T_1)e$	$t_2^2(^1T_2)e$	$t_2e^2(^3A_2)$	$t_2e^2(^1E)$
t_2^3	$a + 2b - 2j$	$-\sqrt{3}i^*$	$\sqrt{3}i^*$	0	$-2h$
$t_2^3(^3T_1)e$		$b + (4/\sqrt{3})c + 2d$ $+g - j$	$-\sqrt{3}h$	$\sqrt{3}i$	$3i^*$
$t_2^3(^1T_2)e$			$b + 2d - g$ $-(2/\sqrt{3})h + j$	$-\sqrt{3}i$	$-i^*$
$t_2e^2(^3A_2)$				$(2/\sqrt{3})c + 2d + e$ $-3f + g + (1/\sqrt{3})h$	$+2h^*$
$t_2e^2(^1E)$					$e + 2d + (2/\sqrt{3})c$ $-g - (h/\sqrt{3}) - f$
t_2^3	$t_2^3(3T_1)e$	$t_2^2(^3T_1)e$	$t_2^2(^1T_2)e$	$t_2e^2(^1A_1)$	$t_2e^2(^1E)$
t_2^3	$a + 2b$	$-3i$	$-5i^*$	$2g + 2h/\sqrt{3}$	$2h/\sqrt{3}$
$t_2^3(^3T_1)e$		$b - j + 2d + g$ $+2h/\sqrt{3}$	$\sqrt{3}h^*$	$-3i$	$-3i$
$t_2^3(^1T_2)e$			$b + 4c/\sqrt{3} + 2d$ $-g + j$	$-i^*$	$+i^*$
$t_2e^2(^1A_1)$				$e + 2d + 2c/\sqrt{3}$ $-g + f - h/\sqrt{3}$	$4c/\sqrt{3} + 2h/\sqrt{3}$
$t_2e^2(^1E)$					$2c/\sqrt{3} + 2d + e - f$ $-g - h/\sqrt{3}$
t_2^3	$t_2^3(3T_1)e$	$t_2^2(^3T_1)e$	$t_2e^2(^3A_2)$		
$t_2^3(^3T_1)e$		$b + 4c/\sqrt{3} + 2d$ $-2g - j$		$2\sqrt{3}i$	
$t_2e^2(^3A_2)$		$2\sqrt{3}i$		$2c/\sqrt{3} + 2d + e$ $-3f - 2g$ $-2h/\sqrt{3}$	
$t_2^3(^1E)e$					
$t_2^3(^1E)e$					$t_2^3(^1E)e: ^2A_1 = a - 2c/\sqrt{3} + 2d - g - \sqrt{3}h - j$
$t_2^3(^1E)e$					$t_2^3(^1E)e: ^2A_2 = a + 2\sqrt{3}c + 2d - g + h/\sqrt{3} - j$
$t_2^3(^1E)e$					$t_2^3(^1E)e: ^4A_2 = 3b - 3i$
$t_2^3(^1E)e$					$t_2^3(^3T_1)e: ^4T_2 = b + 2d - 2g - 4h/\sqrt{3} - j$

TABLE IV. Electron-electron matrix elements for d^4 electrons. Asterisk denotes the change in sign with respect to Griffith's matrix elements.

3T_1	t_2^1	$t_2^1({}^2T_1)e$	$t_2^1({}^2T_2)e$	$t_2^1({}^6T_1)e^2({}^4A_1)$	$t_2^1({}^6T_1)e^2({}^4E)$	$t_2^1({}^4T_2)e^2({}^4A_2)$	$t_2e^3({}^6E)$
$\frac{1}{4}$	$a + 5b - 3j$	$-\sqrt{2}i$	$-\sqrt{6}i$	$\sqrt{2}g + \frac{\sqrt{2}}{\sqrt{3}}h^*$	$-\frac{2\sqrt{2}}{\sqrt{3}}h^*$	0	0
$t_2^1({}^2T_1)e$		$a + 2b + \sqrt{3}c$	$2c + h$	$+i^*$	$-i^*$	$\sqrt{3}i$	$\sqrt{2}h$
		$+3d - 2g$					
		$-\sqrt{3}h - 2j$					
$t_2^1({}^2T_2)e$		$a + 2b + \sqrt{3}c$		$-\sqrt{3}i^*$	$-\sqrt{3}i^*$	$5i$	$+\sqrt{2}g$
		$+3d - 2g$					
		$-\frac{1}{\sqrt{3}}h$					
$t_2^1({}^6T_1)e^2({}^4A_1)$				$b + \frac{4}{\sqrt{3}}c + 4d$	$-\frac{4}{\sqrt{3}}c - \frac{2}{\sqrt{3}}h$	0	$\sqrt{6}i^*$
				$+e + f - 2g$			
				$-\frac{2}{\sqrt{3}}h - j$			
$t_2^1({}^6T_1)e^2({}^4E)$					$b + \frac{4}{\sqrt{3}}c + 4d$	$-2h^*$	$-\sqrt{6}i^*$
					$+e - f - 2g$		
					$-\frac{2}{\sqrt{3}}h - j$		
$t_2^1({}^4T_2)e^2({}^4A_2)$						$b + \frac{4}{\sqrt{3}}c + 4d$	$\sqrt{2}i$
						$+e - 3f - 2g$	
						$-\frac{2}{\sqrt{3}}h + j$	
$t_2e^3({}^6E)$							$\frac{1}{\sqrt{3}}c + 3d + 3e$
							$-5f - 2g - \frac{2}{\sqrt{3}}h$
1T_2	t_2^1	$t_2^1({}^2T_1)e$	$t_2^1({}^2T_2)e$	$t_2^1({}^6T_1)e^2({}^4A_2)$	$t_2^1({}^6T_2)e^2({}^4E)$	$t_2^1({}^4T_2)e^2({}^4A_1)$	t_2e^3
$\frac{1}{4}$	$a + 5b - j$	$\sqrt{6}i^*$	$-5\sqrt{2}i$	0	$-\frac{2\sqrt{2}}{\sqrt{3}}h^*$	$\sqrt{2}g + \frac{\sqrt{2}}{\sqrt{3}}h^*$	0
$t_2^1({}^2T_1)e$		$a + 2b + \sqrt{3}c$	$-2c - h^*$	$\sqrt{3}i$	$-\sqrt{3}i$	$-\sqrt{3}i$	$-\sqrt{2}h^*$
		$+3d - \sqrt{3}h - 2j$					
$t_2^1({}^2T_2)e$		$a + 2b + \sqrt{3}c$		$-3i^*$	$+5i^*$	$-5i^*$	$\sqrt{2}g + \frac{2\sqrt{2}}{\sqrt{3}}h$
		$+3d + \sqrt{3}h$					
$t_2^1({}^6T_1)e^2({}^4A_2)$				$b + \frac{4}{\sqrt{3}}c + 4d + e$			
				$-3f + 2g + \frac{2}{\sqrt{3}}h$	$-2\sqrt{3}h$	0	$-3\sqrt{2}i^*$
				$-j$			
$t_2^1({}^6T_2)e^2({}^4E)$					$b + \frac{4}{\sqrt{3}}c + 4d + e$	$-\frac{4}{\sqrt{3}}c - \frac{2}{\sqrt{3}}h$	$+\sqrt{2}i^*$
					$-f - 2g - \frac{2}{\sqrt{3}}h$		
					$+j$		
$t_2^1({}^4T_2)e^2({}^4A_1)$						$b + \frac{4}{\sqrt{3}}c + 4d$	$+\sqrt{2}i^*$
						$+e + f - 2g$	
						$-\frac{2}{\sqrt{3}}h + j$	
t_2e^3							$\frac{5}{\sqrt{3}}c + 3d + 3e$
							$-5f + \frac{4}{\sqrt{3}}h$

TABLE IV. (Continued)

$t_1^1 A_1$	t_2^1	$t_2^1 ({}^2 E) e$	$t_2^1 ({}^1 A_1) e^2 ({}^1 A_1)$	$t_2^1 ({}^1 E) e^2 ({}^1 E)$	e^4
t_2^1	$2a + 4b$	$-4\sqrt{3}i$	$2\sqrt{2}g + \frac{2\sqrt{2}}{\sqrt{3}}h$	$+\frac{2\sqrt{2}}{\sqrt{3}}h^*$	0
$t_2^1 ({}^2 E) e$		$3b + \sqrt{3}c + 3d$ $+ 2\sqrt{3}h$	$-4\sqrt{3}i$	$-2\sqrt{3}i^*$	0
$t_2^1 ({}^1 A_1) e^2 ({}^1 A_1)$			$a + \frac{4}{\sqrt{3}}c + 4d$ $+ e + f - 2g$ $-\frac{2}{\sqrt{3}}h + 2j$	$+\frac{8}{\sqrt{3}}c + \frac{4}{\sqrt{3}}h^*$ $-f - 2g - \frac{2}{\sqrt{3}}h$ $-j$	$\sqrt{6}g + \sqrt{2}h$
$t_2^1 ({}^1 E) e^2 ({}^1 E)$				$a + \frac{4}{\sqrt{3}}c + 4d + e$	$+ 2\sqrt{2}h^*$
e^4					$6e - 10f$
t_E	t_2^1	$t_2^1 ({}^2 E) e$	$t_2^1 ({}^1 E) e^2 ({}^1 A_1)$	$t_2^1 ({}^1 A_1) e^2 ({}^1 E)$	$t_2^1 ({}^1 E) e^2 ({}^1 E)$
t_2^1	$2a + 4b - 3j$	$2\sqrt{3}i$	$\sqrt{2}g + \frac{\sqrt{2}}{\sqrt{3}}h^*$	$-\frac{2}{\sqrt{3}}h$	$-\frac{4}{\sqrt{3}}h^*$
$t_2^1 ({}^2 E) e$		$3b + \sqrt{3}c + 3d$	$-\sqrt{6}i^*$	$-4\sqrt{3}i$	0
$t_2^1 ({}^1 E) e^2 ({}^1 A_1)$			$a + \frac{4}{\sqrt{3}}c + 4d$ $+ e + f - 2g$ $-\frac{2}{\sqrt{3}}h - j$	$\frac{4\sqrt{2}}{\sqrt{3}}c + \frac{2\sqrt{2}}{\sqrt{3}}h^*$	$-\frac{4\sqrt{2}}{\sqrt{3}}c - \frac{2\sqrt{2}}{\sqrt{3}}h$
$t_2^1 ({}^1 A_1) e^2 ({}^1 E)$				$a + \frac{4}{\sqrt{3}}c + 4d + e$ $-f - 2g - \frac{2}{\sqrt{3}}h$ $+ 2j$	0
$t_2^1 ({}^1 E) e^2 ({}^1 E)$					$a + \frac{4}{\sqrt{3}}c + 4d$ $+ e - f - 2g - \frac{2}{\sqrt{3}}h - j$
$t_1^1 T_1$	$t_2^1 ({}^2 T_1) e$	$t_2^1 ({}^2 T_2) e$	$t_2^1 ({}^1 T_2) e^2$	$t_2^1 e^3$	
$t_2^1 ({}^2 T_1) e$	$a + 2b + \sqrt{3}c + 3d$ $+ \sqrt{3}h - 2j$	$2c + h$	$\sqrt{3}i^*$	$\sqrt{2}h$	
$t_2^1 ({}^2 T_2) e$		$a + 2b + \sqrt{3}c$ $+ 3d - \sqrt{3}h$	$-5i^*$	$\sqrt{2}g$	
$t_2^1 ({}^1 T_2) e^2$			$b + \frac{4}{\sqrt{3}}c + 4d$ $+ e - f - 2g$ $-\frac{2}{\sqrt{3}}h + i$	$-\sqrt{2}i^*$	
$t_2^1 e^3$				$\frac{c}{\sqrt{3}} + 3d + 3e - 5f - \frac{4}{\sqrt{3}}h$	
$t_2^3 T_2$	$t_2^1 ({}^2 T_1) e$	$t_2^1 ({}^2 T_2) e$	$t_2^1 ({}^1 T_1) e^2 ({}^1 A_2)$	$t_2^1 ({}^1 T_1) e^2 ({}^1 E)$	$t_2^1 e^3$
$t_2^1 ({}^2 T_1) e$	$a + 2b + \sqrt{3}c$ $+ 3d - 2g - \frac{h}{\sqrt{3}}$ $- 2j$	$-2c - h^*$	$\sqrt{2}i$	i^*	$-\sqrt{2}h^*$
$t_2^1 ({}^2 T_2) e$		$a + 2b + \sqrt{3}c$ $+ 3d - 2g - \sqrt{3}h$	$-\sqrt{6}i^*$	$\sqrt{3}i$	$\sqrt{2}g + \frac{2\sqrt{2}h}{\sqrt{3}}$
$t_2^1 ({}^1 T_1) e^2 ({}^1 A_2)$			$b + \frac{4}{\sqrt{3}}c + 4d$ $+ e - 3f - j$	$-\frac{2\sqrt{2}}{\sqrt{3}}h^*$	$-2\sqrt{3}i^*$
$t_2^1 ({}^1 T_1) e^2 ({}^1 E)$				$b + \frac{4}{\sqrt{3}}c + 4d$ $+ e - f - 2g$ $-\frac{2}{\sqrt{3}}h - j$	$\sqrt{6}i$
$t_2^1 e^3$				$\frac{5}{\sqrt{3}}c + 3d + 3e - 5f - 2g - \frac{2}{\sqrt{3}}h$	

TABLE IV. (Continued)

$t_2^3(1A_1)e$	$t_2^3(\ell E)e$	$t_2^3(\ell E)e^2(\ell A_2)$	$t_2^3(\ell E)e^2(\ell A_2)$	$t_2^3(1A_1)$	$t_2^3(\ell E)e$	$t_2^3(\ell E)e^2(\ell E)$
$t_2^3(1A_1)e$	$3b + \sqrt{3}c + 3d$	$-\frac{4}{\sqrt{3}}h$	0	$t_2^3(\ell E)e$	$3b + \sqrt{3}c + 3d$	$2\sqrt{3}i^*$
	$+g + \frac{h}{\sqrt{3}} - 3j$				$-2\sqrt{3}h$	
$t_2^3(\ell E)e$	$3b + \sqrt{3}c + 3d$	$-\sqrt{6}i^*$		$t_2^3(1E)e^2(\ell E)$		$a + \frac{4}{\sqrt{3}}c + 4d$
	$-2g - \frac{2}{\sqrt{3}}h$					$+e - f - 2g$
$t_2^3(1E)e^2(1A_1)$		$a + \frac{4}{\sqrt{3}}c + 4d$				$-\frac{2}{\sqrt{3}}h - j$
		$+e - 3f - 2g - \frac{2}{\sqrt{3}}h - j$		$t_2^3(\ell E)e$	$3A_1 = 3b + \sqrt{3}c + 3d$	
$3A_2$	$t_2^3(\ell E)e$	$t_2^3(1A_1)e^2(\ell A_2)$			$-2g - 4h/\sqrt{3}$	
$t_2^3(\ell E)e$	$3b + \sqrt{3}c$	$-4\sqrt{3}i$		$t_2^3(1A_2)e$	$5E = 3b + \sqrt{3}c + 3d$	
	$+3d - 2g$				$-3g - \sqrt{3}h - 3j$	
$t_2^3(1A_1)e^2(\ell A_2)$		$a + \frac{4}{\sqrt{3}}c + 4d$		$t_2^3(1T_1)e^2(\ell A_2)$	$5T_2 = b + 4c/\sqrt{3} + 4d$	
		$+e - 3f - 2g - \frac{2}{\sqrt{3}}h + 2j$			$+e - 3f - 4g$	
					$-4h/\sqrt{3} - j$	

Although we have followed consistently Griffith's phase conventions, we have not been able to trace out why we disagree in sign in some of our matrix elements from those listed by Griffith.³

As for the matrix elements of the complementary states d^{10-n} ($n=2, 3, 4, 5$), the nondiagonal matrix

elements remain the same as in d^n matrices but the diagonal matrix elements of d^{10-n} states differ from the corresponding ones of d^n by a function which is a linear combination of V_i 's. The straightforward but tedious group-theoretical method yields the general expression,

$$\begin{aligned} & \langle t_2^{6-m}(S_1\Gamma_1)e^{4-l}(S_2\Gamma_2)STM_S M_\Gamma | (e^2/r_{12}) | t_2^{6-m}(S_1\Gamma_1)e^{4-l}(S_2\Gamma_2)STM_S M_\Gamma \rangle \\ & - \langle t_2^m(S_1\Gamma_1)e^l(S_2\Gamma_2)STM_S M_\Gamma | (e^2/r_{12}) | t_2^m(S_1\Gamma_1)e^l(S_2\Gamma_2)STM_S M_\Gamma \rangle \\ & = (3-m)V_1 + 4(3-m)V_2 + (24 - 4m - 6l)(V_3/\sqrt{3} + V_4) + (6 - 3l)V_5 \\ & + (5l - 10)V_6 + (2m + 3l - 12)V_7 + (2m + 3l - 12)V_8/\sqrt{3} - 2(3-m)V_{10}, \quad (1) \end{aligned}$$

where the integers m and l are connected to n by the relation

$$m + l = n \text{ or } 10 - n. \quad (2)$$

In Eq. (1) t_2 represents the orbitals ξ , η , and ζ and e represents the orbitals θ and ϵ . S_i and S are the total spin quantum numbers and Γ_i 's and Γ are the irreducible representations of the cubic group. The difference between the diagonal element of d^n and d^{10-n} as given by Eq. (1) reduces, as expected, for the pure d -electron case to

$$\begin{aligned} & \langle t_2^{6-m}(S_1\Gamma_1)e^{4-l}(S_2\Gamma_2)STM_S M_\Gamma | (e^2/r_{12}) | t_2^{6-m}(S_1\Gamma_1)e^{4-l}(S_2\Gamma_2)STM_S M_\Gamma \rangle \\ & - \langle t_2^m(S_1\Gamma_1)e^l(S_2\Gamma_2)STM_S M_\Gamma | (e^2/r_{12}) | t_2^m(S_1\Gamma_1)e^l(S_2\Gamma_2)STM_S M_\Gamma \rangle = (45A - 70B + 35C) - (9A - 14B + 7C)(m + l), \quad (3) \end{aligned}$$

where A , B , and C are the standard Racah parameters. One notes that in the case of pure d orbitals, the expression (3) depends only on the sum $(m + l)$ which according to Eq. (2) is n or $10 - n$ and hence, for a given n (with whatever appropriate values of the set m, l) the difference between the diagonal elements in Eq. (3) is constant. The above formula is particularly significant since it reveals that the diagonal elements of the d^{10-n} configuration change by different amounts from the corresponding ones for the d^n configuration. As an example, for the configuration d^3 the diagonal element

$$\langle t_2^3(2E)e^0(1E)^2E | (e^2/r_{12}) | t_2^3(2E)e^0(1E)^2E \rangle$$

and the corresponding one in the configuration d^7 differ by the amount

$$[-12(V_3/\sqrt{3} + V_4) - 6V_5 + 10V_6 + 6V_7 + 2\sqrt{3}V_8],$$

whereas the diagonal element

$$\langle t^0(1A_1)e^3(2E)^2E | (e^2/r_{12}) | t^0(1A_1)e^3(2E)^2E \rangle$$

in the configuration d^3 differs from the corresponding one in the d^7 configuration by

TABLE V. Electron-electron matrix elements for d^5 electrons. Asterisk denotes the change in sign with respect to Griffith's matrix elements.

$t_2^2(1A_1)$	$t_2^4(1E)e$	$t_2^3(2E)e^2(1E)$	$t_2^3(4A_2)e^2(3A_2)$	$t_2^2(1E)e^3$
$t_2^4(1E)e$	$2a + 4b + \frac{8}{\sqrt{3}}c + 4d - 2g - 3j$	$-\sqrt{6}i$	0	$g + \frac{5}{\sqrt{3}}h^*$
$t_2^3(2E)e^2(1E)$	$3b + 2\sqrt{3}c + 6d$ $+e - f - 3g$ $-\sqrt{3}h$	$-4h^*$	$\sqrt{6}i^*$	
$t_2^3(4A_2)e^2(3A_2)$		$3b + 2\sqrt{3}c + 6d$ $+e - 3f + 2g + \frac{2}{\sqrt{3}}h - 3j$	0	
$t_2^2(1E)e^3$				$a + \frac{10}{\sqrt{3}}c + 6d$ $+3e - 5f - 3g - \frac{1}{\sqrt{3}}h - j$
$t_2^2(1A_2)$	$t_2^4(1E)e$	$t_2^3(2E)e^2(1E)$	$t_2^3(4A_2)e^2(3A_2)$	$t_2^2(1E)e^3$
$t_2^4(1E)e$	$2a + 4b + 4d$ $-2g - \frac{4}{\sqrt{3}}h$ $-3j$	$\sqrt{6}i$	$g - \sqrt{3}h^*$	
$t_2^3(2E)e^2(1E)$		$3b + 2\sqrt{3}c + 6d$ $+e - f - 3g$ $-\sqrt{3}h$	$-\sqrt{6}i^*$	
$t_2^3(4A_2)e^2(3A_2)$				$a + \frac{2}{\sqrt{3}}c + 6d$ $+3e - 5f - 3g$ $-\frac{5}{\sqrt{3}}h - j$
$t_2^2(1E)$	$t_2^4(1A_1)e$	$t_2^4(1E)e$	$t_2^3(2E)e^2(1A_1)$	$t_2^3(2E)e^2(3A_2)$
$t_2^4(1A_1)e$	$2a + 4b + \frac{4}{\sqrt{3}}c$ $+4d - 2g - \frac{2}{\sqrt{3}}h$	$\frac{4}{\sqrt{3}}c + \frac{2}{\sqrt{3}}h$	$2\sqrt{3}i$	$6i$
$t_2^4(1E)e$		$2a + 4b + \frac{4}{\sqrt{3}}c$ $+4d - 2g$ $-\frac{2}{\sqrt{3}}h - 3j$	$-\sqrt{3}i$	$3i$
$t_2^3(2E)e^2(1A_1)$		$3b + 2\sqrt{3}c + 6d$ $+e - f - 3g$ $-\sqrt{3}h$	0	0
$t_2^3(2E)e^2(3A_2)$		$3b + 2\sqrt{3}c$ $+6d + e - 3f - g$ $-\frac{h}{\sqrt{3}}$	$2\sqrt{2}h$	$-3i^*$
$t_2^3(2E)e^2(1E)$		$3b + 2\sqrt{3}c + 6d$ $+e - f - 3g$ $-\sqrt{3}h$	0	$2\sqrt{6}i$
$t_2^2(1E)e^3$				$a + 2\sqrt{3}c + 6d$ $+3e - 5f - 3g$ $-\sqrt{3}h - j$
$t_2^2(1A_1)e^3$				$a + 2\sqrt{3}c + 6d$ $+3e - 5f - 3g$ $-\sqrt{3}h + 2j$

TABLE V. (*Continued*)

$t_2^3(2E)e^2(3A_2)$	$t_2^3(4A_2)e^2(1E)$	$t_2^4(3T_1)e$	$t_2^3(2T_2)e^2(3A_2)$	$t_2^2(3T_1)e^3$
$3b + 2\sqrt{3}c + 6d$ $+ e - 3f - 4g$ $- \frac{4}{\sqrt{3}}h$	$-2h$	$t_2^4(3T_1)e$	$a + 5b + \frac{2}{\sqrt{3}}c$ $+ 4d - 3g - \sqrt{3}h$ $- 3j$	$-\sqrt{6}i^*$ $g - \frac{1}{\sqrt{3}}h^*$
$t_2^3(4A_2)e^2(1E)$	$3b + 2\sqrt{3}c + 6d$ $+ e - f - 3g$ $- \sqrt{3}h - 3j$	$t_2^3(2T_2)e^2(3A_2)$	$a + 2b + 2\sqrt{3}c$ $+ 6d + e - 3f$ $- 4g - \frac{4}{\sqrt{3}}h$	$-\sqrt{6}i$
		$t_2^2(3T_1)e^3$		$b + \frac{4}{\sqrt{3}}c + 6d$ $+ 3e - 5f - 4g$ $- \frac{4}{\sqrt{3}}h - j$
$t_2^4(3T_1)e$	$t_2^4(3T_1)e$	$t_2^3(2T_1)e^2(3A_2)$	$t_2^2(3T_1)e^3$	
$t_2^3(2T_1)e^2(3A_2)$	$a + 5b + 2\sqrt{3}c$ $+ 4d - 3g - \sqrt{3}h$ $- 3j$	$\sqrt{2}i^*$	$g + \sqrt{3}h^*$	
		$a + 2b + 2\sqrt{3}c$ $+ 6d + e - 3f$ $- 4g - \frac{4}{\sqrt{3}}h$ $- 2j$	$-\sqrt{2}i$	
$t_2^2(3T_1)e^3$				$b + \frac{8}{\sqrt{3}}c + 6d$ $+ 3e - 5f - 4g$ $- \frac{4}{\sqrt{3}}h - j$

$$[-3V_1 - 12V_2 - 6(V_3/\sqrt{3} + V_4) + 3V_5 - 5V_6 \\ + 3V_7 + \sqrt{3}V_8 + 6V_{10}].$$

Also, in the configuration d^3 the diagonal element

$$\langle t_2^2(3T_1)e^1(2E)^2T_1 | (e^2/r_{12}) | t_2^2(3T_1)e^1(2E)^2T_1 \rangle$$

differs from the corresponding diagonal element in the d^7 configuration by

$$[-V_1 - 4V_2 - 10(V_3/\sqrt{3} + V_4) - 3V_5 + 5V_6 \\ + 5V_7 + 5V_8/\sqrt{3} + 2V_{10}].$$

It is clear from the above examples that the various diagonal elements are changed by the different amounts in going from the d^n to d^{10-n} configuration. On the other hand, if pure *d* orbitals are involved, all the diagonal elements of the d^3 configuration differ from the corresponding diagonal elements of the d^7 configuration by the constant amount $(-18A + 28B - 14C)$ which agrees with the result given by Griffith.³ Thus, in general the present results from our improved treatment differ from the corresponding results in the simplified theory of the pure *d* orbitals where a constant difference has been well known. The significance of the new diagonal elements will be made clear in Sec. III.

It must be recalled that in cubic-crystal fields the diagonal matrix elements for the states $|t_2^2e^3\rangle$

are further admixed, as usual, by the crystal field term $(0.4q - 0.6p)\Delta$, where $\Delta = 10Dq$ is the cubic-field splitting parameter. The splitting parameter Δ is positive for the octahedral symmetry and in that case the t_2 level lies below the *e* level. On the other hand, in the case of tetrahedral symmetry it has been explained by Griffith³ that the parameter Δ changes sign thereby inverting t_2 and *e* levels. Also the diagonal matrix elements of the d^n configuration are related to those of d^{10-n} configuration in a given symmetry (octahedral or tetrahedral). This is a very important result concerning our improved theory since the diagonal elements no longer change by the same amount as expressed mathematically by Eq. (1). Thus, in several cases, based solely on this type of change in the diagonal elements, the energy levels in the new treatment are expected to be different and certain levels which are degenerate in the old treatment are now expected to have split components in the improved new treatment.

III. IMPACT OF IMPROVED MATRICES ON EXISTING RESULTS

At first glance, the full import of the matrices derived in Sec. II may not be obvious owing to the fact that one now has eleven parameters

TABLE V. (Continued)

$t_1^2(1T_1)e$	$t_2^2(1T_1)e$	$t_2^3(1T_1)e^2(1A_1)$	$t_2^3(2T_1)e^2(1E)$	$t_2^3(2T_1)e^2(3A_2)$	$t_2^3(2T_1)e^2(1E)$	$t_2^3(2T_2)e^2(1E)$	$t_2^3(1T_2)e^3$	$t_2^3(1T_1)e^3$
$t_2^3(2T_2)e$	$a + 5b + \frac{2}{\sqrt{3}}c$ $+ 4d - \sqrt{3}h - 3j$	$-\sqrt{3}h$	$-\frac{\sqrt{6}}{2}i$	$\frac{1}{2}\sqrt{6}i$	$-\frac{1}{2}\sqrt{6}i^*$	$-\frac{3}{\sqrt{2}}i$	$g - \frac{h}{\sqrt{3}}$	
$t_2^3(2T_1)e^2(1A_1)$	$a + 5b + 2\sqrt{3}c$ $+ 4d - 2g$ $-\frac{h}{\sqrt{3}} - j$	$\frac{1}{2}\sqrt{6}i$	$\frac{1}{2}\sqrt{6}i^*$	$\frac{5}{\sqrt{2}}i$	$g + \sqrt{3}h^*$	0	$g - \frac{h}{\sqrt{3}}$	
$t_2^3(2T_1)e^2(1E)$	$a + 2b + 2\sqrt{3}c$ $+ 6d + e + f$ $-3g - \sqrt{3}h - 2j$	0	0	$4c + 2h$	$\frac{\sqrt{6}}{2}i^*$	$-\frac{\sqrt{6}}{2}i^*$	$-\frac{\sqrt{6}}{2}i$	
$t_2^3(2T_2)e^2(1E)$	$a + 2b + 2\sqrt{3}c$ $+ 6d + e - f$ $-3g - \sqrt{3}h - 2j$	0	0	0	$-\frac{\sqrt{6}}{2}i^*$	$-\frac{\sqrt{6}}{2}i^*$	$-\frac{\sqrt{6}}{2}i$	
$t_2^3(2T_2)e^2(3A_2)$	$a + 2b + 2\sqrt{3}c$ $+ 6d + e - f$ $-g - \frac{h}{\sqrt{3}}$	$2h^*$	$\frac{1}{2}\sqrt{6}i$	$2h^*$	$-\frac{\sqrt{6}}{2}i^*$	$-\frac{3}{\sqrt{2}}i^*$	$-\frac{3}{\sqrt{2}}i^*$	
$t_2^3(2T_2)e^2(1E)$	$a + 2b + 2\sqrt{3}c$ $+ 6d + e - f$ $-3g - \sqrt{3}h$	$2h^*$	$\frac{5}{\sqrt{2}}i^*$	$5d$	$-\frac{3}{\sqrt{2}}i^*$	$-\frac{3}{\sqrt{2}}i^*$	$-\frac{3}{\sqrt{2}}i^*$	
$t_2^3(1T_2)e^3$	$b + \frac{8}{\sqrt{3}}c + 6d$ $+ 3e - 5f - 3g$ $-\frac{2h}{\sqrt{3}} + j$			$-g - \sqrt{3}h$	$-g - \sqrt{3}h$	$-g - \sqrt{3}h$	$-g - \sqrt{3}h$	
$t_2^3(3T_1)e^3$					$b + \frac{4}{\sqrt{3}}c + 6d$ $+ 3e - 5f - g$ $-\frac{4}{\sqrt{3}}h - j$			

TABLE V. (Continued)

t_1^4	t_2^4	t_3^4	$t_4^4(1T_1)e^0$	$t_5^4(1T_1)e$	$t_6^4(1T_1)e^2(1A_2)$	$t_7^4(1T_1)e^0(1E)$	$t_8^4(1T_2)e^2(1A_1)$	$t_9^4(1T_2)e^0(1E)$	$t_{10}^4(1T_1)e^3$	$t_{11}^4(1T_1)e^3$	$t_{12}e^4$
$2e+8d$	$3/2j^*$		$\sqrt{2}i$	0	$-2h^*$	$2g+\frac{2h}{\sqrt{3}}$	$\frac{2h}{\sqrt{3}}$	0	0	0	0
$-4j$					$\frac{i}{\sqrt{2}}^*$	$-\frac{\sqrt{6}}{2}i$	$\frac{3}{\sqrt{2}}i^*$	$\frac{3}{\sqrt{2}}i^*$	0	$g+\sqrt{3}h^*$	0
$t_5^4(1T_1)e$			$a+3b+2/\sqrt{3}c$	$\sqrt{3}h^*$							
			$+4d+\sqrt{3}h-3j$								
$t_5^4(1T_2)e$			$a+5b+\frac{2}{\sqrt{3}}c$	$\frac{3}{\sqrt{2}}i^*$	$-\frac{\sqrt{6}}{2}i^*$	$\frac{5}{\sqrt{2}}i$	$-\frac{5}{\sqrt{2}}i$	$g-\frac{h}{\sqrt{3}}^*$	0	0	0
$t_6^4(1T_1)e^2(1A_2)$			$+4d-2g-\sqrt{3}h-j$								
			$a+2b+2\sqrt{3}c$	$2h^*$	0	0		$-\frac{3}{\sqrt{2}}i^*$	$-\frac{1}{\sqrt{2}}i$	0	
			$+6d+e-3f$								
			$-g-\frac{h}{\sqrt{3}}-2j$								
$t_7^4(1T_1)e^2(1E)$			$a+2b+2\sqrt{3}c$	$-4c-2h^*$	0	$-\frac{\sqrt{6}}{2}i$	$\frac{\sqrt{6}}{2}i^*$		$-2h^*$		
			$+6d+e-f$								
			$-3g-\sqrt{3}h-2j$								
$t_8^4(1T_2)e^2(1A_1)$					$a+2b+2\sqrt{3}c$	0	$-\frac{5}{\sqrt{2}}i^*$	$-\frac{3}{\sqrt{2}}i$	$2g+\frac{2}{\sqrt{3}}h$		
					$+6d+e+f$						
					$-3g-\sqrt{3}h$						
$t_9^4(1T_2)e^2(1E)$					$a+2b+2\sqrt{3}c$	$-\frac{5}{\sqrt{2}}i^*$		$\frac{3}{\sqrt{2}}i$	$-\frac{2}{\sqrt{3}}h$		
					$+6d+e-f$						
					$-3g-\sqrt{3}h$						
$t_{10}^4(1T_1)e^3$					$b+\frac{4}{\sqrt{3}}c$		$\sqrt{3}h^*$		$-\sqrt{2}j^*$		
					$+6d+3e-5f$						
					$-3g-\frac{4}{\sqrt{3}}i+j$						
$t_{11}^4(1T_1)e^3$											
$t_{12}e^4$									$\frac{4}{\sqrt{3}}c+4d+6e$		
									$+3e-5f-g$		
									$+\frac{2}{\sqrt{3}}h-j$		
									$-\frac{10}{\sqrt{3}}f-2g-\frac{2}{\sqrt{3}}h$		
$t_5^4(1A_2)e^2(3A_2)$: ${}^4A_1=3b+2\sqrt{3}c+6d+e+f$									$t_5^4(1A_2)e^2(3A_2)$: ${}^4A_1=3b+2\sqrt{3}c+6d+e-3f-6g$		
									$-3g-\sqrt{3}h-3j$		
									$-2\sqrt{3}h-3j$		

(V_1, V_2, \dots, V_{10} , and Δ) replacing four parameters (A, B, C , and Δ) of the old theory. The large number of parameters makes the theory apparently less attractive, but it is important to note that it includes the effect of the surroundings in the correct way. The new theory, however, is very significant since it has been able to (i) test the calculations¹ made on GaAs:Cr²⁺ and GaAs:Cr³⁺ and make comparisons, (ii) give correct group-theoretical assignments to the observed energy levels of the impurity in solids and predict the values of the Coulomb and exchange interaction constants which are otherwise not possible to know from any other source, and (iii) remove the accidental degeneracy inherent in the B, C, Δ theory. It is conceivable that, in due course, from the applications of the present matrices to a variety of physical problems, the full significance of the theory and the generality of the present superior formalism will become even more obvious. Only the first two points will be discussed in the following section since the third point has already been discussed briefly in Secs. I and II.

A. GaAs:Cr²⁺ and GaAs:Cr³⁺ energies

The impurities Cr²⁺3d⁴ and Cr³⁺3d³ occupy the tetrahedral site substituting Ga in GaAs. As mentioned in Sec. I, Hemstreet and Dimmock¹ have recently performed calculations for these systems by modifying the free-ion one-electron orbitals of t_2 and e symmetry in such a way that their normalization constants were altered by means of the parameters R_{ee} , R_{tt} , and R_{et} which were deduced from the $X\alpha$ calculations. We have used the matrix elements listed in Tables III and IV for d³ and d⁴ electrons to verify the earlier calculations¹ for GaAs:Cr³⁺ and GaAs:Cr²⁺. Repetition of the calculations yields general agreement of our results with those of Hemstreet and Dimmock.¹ However, there are some minor differences [see Fig. (1)]: (i) their two 1T_1 levels of energies 0.74 and 0.84 eV give energies 0.80 and 1.02 eV in our calculations, (ii) 5T_1 in Ref. 1 should have been designated 3T_1 , and (iii) 1E with energy 1.45 eV and 3T_1 with energy 1.33 eV in Ref. 1 should have been originated from the configuration e^2t^2 instead of from the configuration t^4 . The above slight differences may be due to some errors in their d⁴ matrix elements.

We have also calculated the energy level for GaAs:Cr³⁺ and compared our values with those obtained earlier.¹ Figure 2 depicts our calculations where comparison has also been made with the results of Ref. 1 (keeping the same values of the parameters involved as in Ref. 1). Our results [Fig. 2(b)] are in good agreement with earlier results [Fig. 2(a)] except that their 4T_1 at 0.7 eV and 2T_2 at 0.95 eV should now both be 2T_1 .

B. Refined interpretation of the experimental spectra and deduction of exchange and Coulomb-interaction constants

A short report⁴ on the application of the present refined treatment to the analysis of the recently observed¹⁵ fine optical spectra of MgF₂:Co²⁺d⁷ and MgF₂:Mn²⁺d⁵ has already been presented. Here we only briefly state the concluding remarks in order to further justify the importance of the refined matrices given in Tables II-V.

Sibley and co-workers¹⁵ and others have performed excellent optical experiments which yield many sharp and abundant lines of the transition-metal ions in solids. They have observed not only the spin quartet states but also many hitherto unobserved spin doublets by lifting the spin forbiddenness of the excitations through exchange interactions with the color centers. These abundant and fine lines offer an opportunity for their interpretation by means of the refined treatment presented here and also at the same time obtain the values of the parameters V_i 's along with the more accurate value of Δ by solving the inverse eigenvalue problem. We find that in the case of MgF₂:Co²⁺ [using Table III and Eq. (1)] some of the previous tentative assignments¹⁵ of the lines based on the three-parameter theory are now altered. The line previously designated as $^2E_g(^2G)$ is found to be really a mixture of $^2E_g(^2G)$ and $^2T_{1g}(^2G)$; $^2T_{1g}(^2G)$ is really $^2T_{2g}(^2G)$. The deduced values of the interaction parameters and the splitting parameter Δ in eV are: $V_1 - V_2 = 1.616$, $V_1 - V_4 = 1.702$, $V_1 - V_5 = 0.302$, $V_3 = 0.338$, $V_6 = 1.053$, $V_7 = 0.399$, $V_8 = 0.239$, $V_9 = 0.156$, $V_{10} = 0.773$, and $\Delta = -0.899$. Compared to these values, our calculated free-ion values (using Clementi's wave functions¹⁶) are: $V_1 - V_2 = 2.097$, $V_1 - V_4 = 2.097$, $V_1 - V_5 = 0$, $V_3 = 0.543$, $V_6 = 1.205$, $V_7 = 0.735$, $V_8 = 0.271$, $V_9 = 0.271$, and $V_{10} = 1.049$ eV.

As for Mn²⁺3d⁵ in MgF₂, for the second, sixth, eighth, and ninth lines, the assignments given in Ref. 15 as $^4T_{1g}(^4G)$, $^4T_{1g}(^4P)$, $^4T_{1g}(^4F)$, and $^4T_{2g}(^4F)$ turn out to be $^4T_{2g}(^4G)$, $^2T_{2g}(^2D)$, $^2A_{1g}(^2G)$, and $^4T_{1g}(^4F)$, respectively. The deduced values of exchange and Coulomb parameters and the refined value of the cubic-field splitting parameter in this case are: $V_1 - V_2 = 1.385$, $V_1 - V_4 = 1.479$, $V_1 - V_5 = 0.080$, $V_3 = 0.306$, $V_6 = 0.747$, $V_7 = 0.338$, $V_8 = 0.196$, $V_9 = 0.268$, $V_{10} = 0.755$, and $\Delta = 0.708$ eV, which compare with our calculated free-ion values (using Clementi's wave functions¹⁶) of $V_1 - V_2 = 1.900$, $V_1 - V_4 = 1.900$, $V_1 - V_5 = 0$, $V_3 = 0.491$, $V_6 = 1.092$, $V_7 = 0.667$, $V_8 = 0.245$, $V_9 = 0.245$, and $V_{10} = 0.950$ eV.

Thus, the refined matrix elements are useful to analyze the spectra of ions in solids particularly when abundant and sharp lines are available from experiments. The analysis yields the Coulomb and

exchange integrals along with the refined values of Δ . Moreover, the symmetry assignments of lines are deduced and these are expected to be correct since the treatment is based entirely on group theory. Also, this analysis will stimulate further ex-

periments to observe more and sharper experimental lines and also further encourage the development of the first-principles theory to explain the deduced interaction and crystal-field splitting parameters.

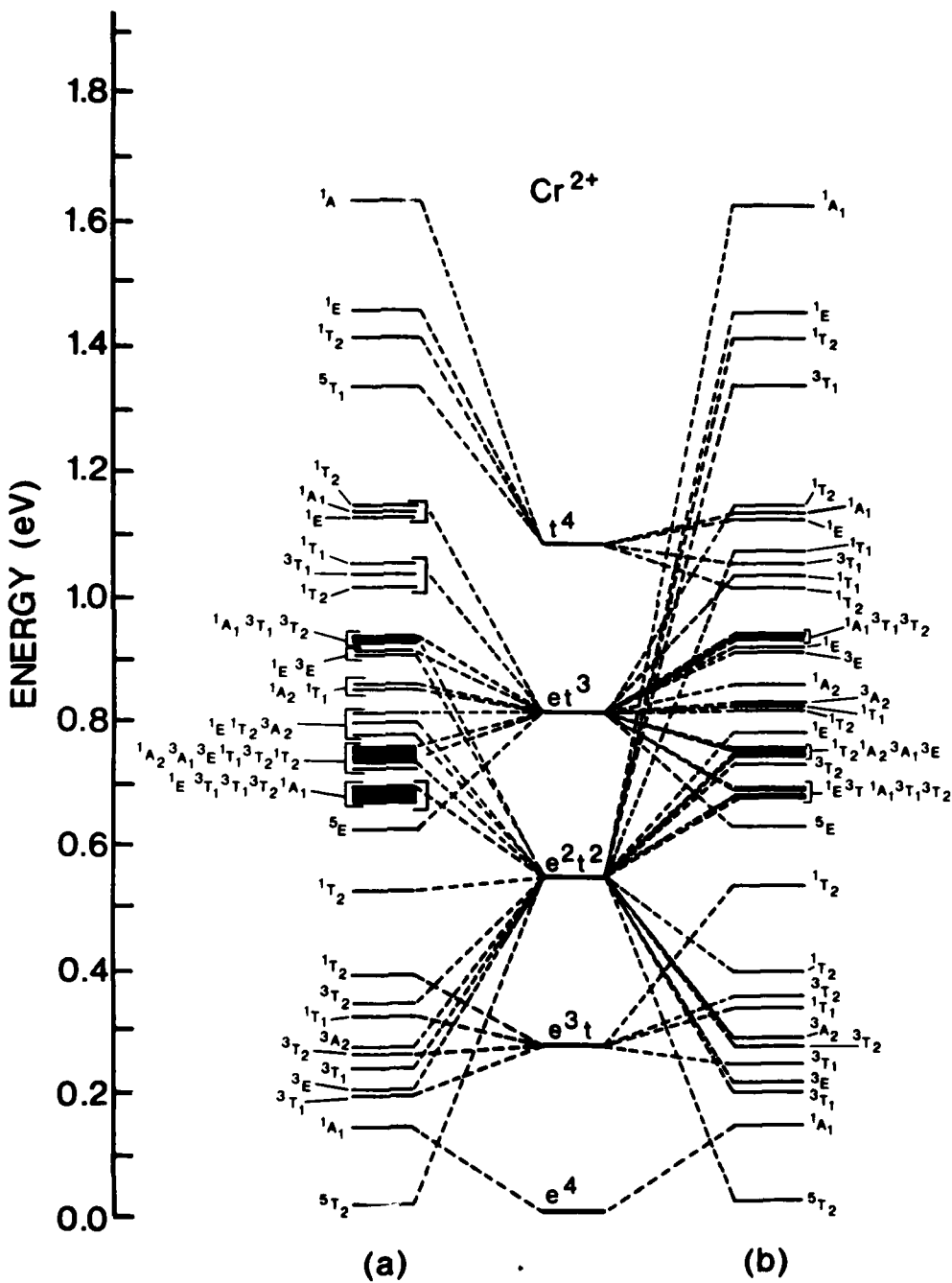


FIG. 1. Shows the energy levels of GaAs:Cr²⁺ (a) calculations by Hemstreet and Dimmock (Ref. 1) and (b) present calculations employing d^4 matrices of octahedral symmetry from Table IV. The values of the parameters A , B , C , Δ , R_{ee} , R_{et} , and R_{tt} in both cases are kept the same as in Ref. 1.

IV. DISCUSSION AND CONCLUSION

The need to improve and generalize the Tanabe-Sugano² interaction matrices has been justified in Secs. I and III in order to eliminate the defects present in the previous treatment which is based on the consideration that the d -electron transition-metal ions in solids contain pure d orbitals. The improved treatment in Sec. II incorporates the solid-state effects adopting group-theoretical techniques and is useful for analyzing the experimental

results more accurately than before, particularly when abundant and fine lines are available through experiments. Such analysis in the present investigation has provided not only the definite group-theoretical assignments of the observed lines but also the (hitherto unknown) values of the Coulomb and exchange interaction constants and refined value of Δ . Also, the present treatment examines and verifies the existing calculations¹ (see Sec. III) on GaAs:Cr²⁺ and GaAs:Cr³⁺. Furthermore, the improved matrix elements (Tables II-V) can be used

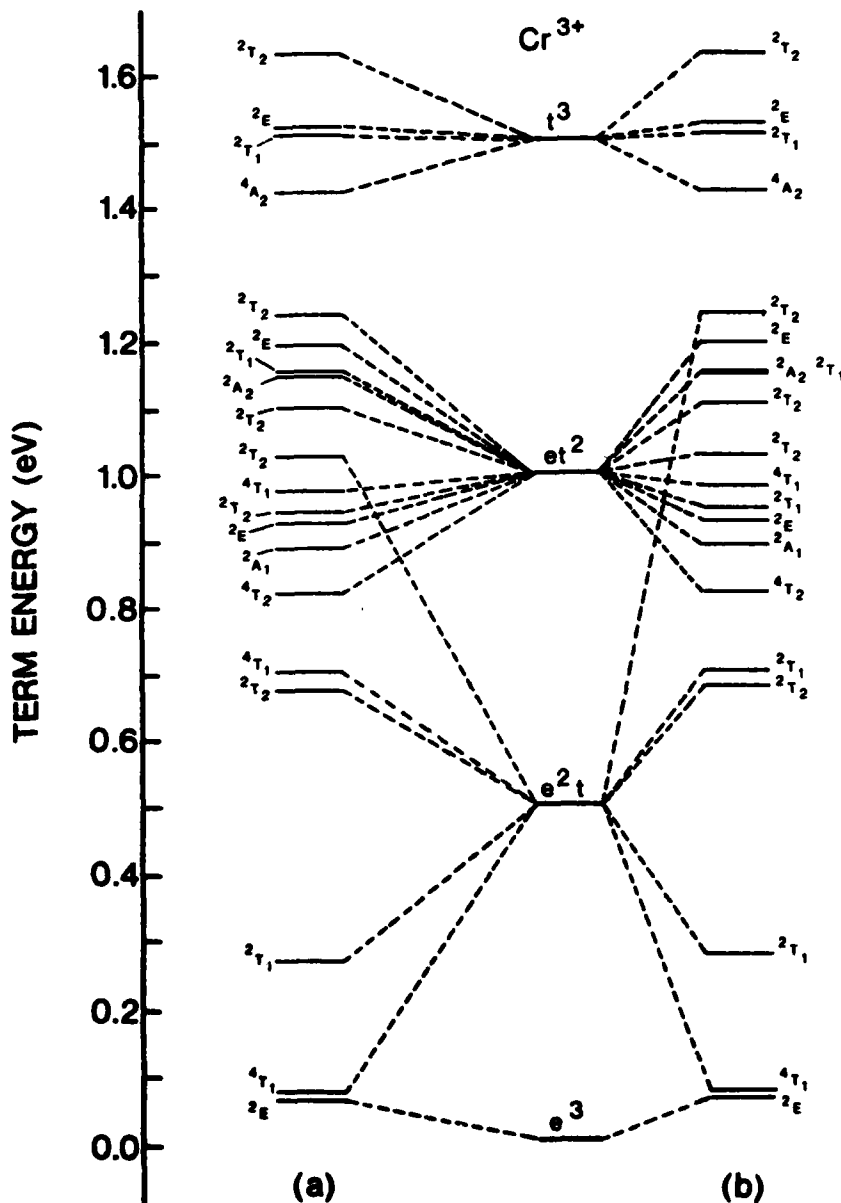


FIG. 2. Energy levels of GaAs:Cr³⁺; (a) Hemstreet and Dimmock's calculations (Ref. 1) and (b) present calculations using d^3 matrices of octahedral symmetry from Table III. The values of the parameters A , B , C , Δ , R_{ee} , R_{et} , and R_{et} are those of Ref. 1.

to explain easily the well-known experimental fact that $^4A_{1g}$ and 4E_g for $Mn^{2+}3d^5$ are different lines which according to B, C, Δ theory are degenerate. In other words, certain lines which are accidentally degenerate in the B, C, Δ theory are resolved in the improved theory.

The present theory is still approximate since no consideration has been given for the spin-orbit interaction and for something equivalent to what is known as the Trees correction¹⁷⁻¹⁹ which deals with the orbit-orbit interaction and because it includes interactions only from a limited number of configurations. With extra efforts, however, it is possible to make such corrections to the results calculated in the present framework. Nonetheless, the improvements obtained in the present study especially in terms of generality, are significant. It is hoped that the present treatment will be ex-

tended appropriately to various other cases⁵ where the experimental results are in poor agreement with the theory. Also, it is expected that this work will provide the necessary stimulus to experimentalists to observe more refined and abundant lines in the spectra and to the theorists to make the first-principles calculations to explain the observed results.

ACKNOWLEDGMENTS

The support of this research by Contract No. N0001478C0732 from the U. S. Office of Naval Research is gratefully acknowledged. Two authors (R.R.S. and S.S.) thank Dr. Hemstreet and Dr. Dimmock for communicating their results prior to publication. One of the authors (M. H. de A. Viccaro) would like to acknowledge a research fellowship from CNPq—Brazil.

¹L. Hemstreet and J. Dimmock, Phys. Rev. B 20, 1527 (1979).

²Y. Tanabe and S. Sugano, J. Phys. Soc. Jpn. 9, 753 (1954); 9, 766 (1954). The Clebsch-Gordan coefficient $\langle T_1\beta T_1\beta | T_1T_1Ev \rangle$ listed in Table I of the first reference (p. 758) is in error; it should read $1/\sqrt{2}$ instead of $1/\sqrt{1}$.

³J. S. Griffith, *The Theory of Transition-Metal Ions* (Cambridge University, Cambridge, New York, 1961).

⁴R. R. Sharma and S. Sundaram, Solid State Commun. 33, 381 (1980); Bull. Am. Phys. Soc. 24, 255 (1979).

⁵J. Ferguson, in *Progress in Inorganic Chemistry*, edited by S. Lippard, (Interscience, New York, 1970), Vol. 12, p. 159; see also the references cited therein.

⁶G. Racah, Phys. Rev. 62, 438 (1942); 63, 367 (1942); 76, 1352 (1949).

⁷R. Finkelstein and J. H. Van Vleck, J. Chem. Phys. 8, 790 (1940).

⁸C. J. Ballhausen, *Introduction to Ligand Field Theory* (McGraw-Hill, New York, 1962).

⁹D. S. McClure, *Solid State Physics*, edited by F. Seitz and D. Turnbull (Academic, New York, 1959), Vol. 9,

p. 399.

¹⁰M. T. Hutchings, *Solid State Physics*, edited by F. Seitz and D. Turnbull (Academic, New York, 1964), Vol. 16, p. 277.

¹¹T. M. Dunn, D. S. McClure, and R. G. Pearson, *Some Aspects of the Crystal Field Theory* (Harper and Row, New York, 1965).

¹²K. W. H. Stevens, Proc. R. Soc. London A 219, 542 (1953).

¹³L. J. Heidt, G. F. Koster, and A. M. Johnson, J. Am. Chem. Soc. 80, 6471 (1958).

¹⁴S. Koide and M. H. L. Pryce, Philos. Mag. 3, 607 (1958).

¹⁵S. I. Yun, L. A. Kappers, and W. A. Sibley, Phys. Rev. B 8, 773 (1973).

¹⁶E. Clementi, IBM J. Res. Dev. 9, 2 (1965).

¹⁷R. E. Trees, Phys. Rev. 82, 683 (1951); 83, 756 (1951); 84, 1089 (1951).

¹⁸G. Racah, Phys. Rev. 85, 382 (1952).

¹⁹F. Rohrlick, Phys. Rev. 101, 69 (1956).

matrix of dimension (43×43) and the experimental energy values [5] to deduce, in units of cm^{-1} , $V_1 - V_2 = 11,176$, $V_1 - V_4 = 11,931$, $V_1 - V_5 = 647$, $V_3 = 2469$, $V_6 = 6026$, $V_7 = 2725$, $V_8 = 1584$, $V_9 = 2164$, $V_{10} = 6093$ (and $Dq = 571$) which compare with the respective free-ion values calculated using Clementi's wave-functions [8], in cm^{-1} 15,328, 15,328, 0, 3958, 8806, 5378, 1979, 1979, 7664 (with the calculated free-ion value $V_1 = 195,437 \text{ cm}^{-1}$). Again, there are no values available for V_i 's from other sources for further comparison; our Dq value, however, lies close to the Dq value for Mn^{2+} in other crystals [1]. We have also obtained assignments of the lines which do not completely agree with the tentative assignments [9] given by Yun *et al.* [5]; in particular, the second, sixth, eighth, and ninth lines come out to be ${}^4T_{2g}({}^4G)$, ${}^2T_{2g}({}^2D)$, ${}^2A_{1g}({}^2G)$ and ${}^4T_{1g}({}^4F)$ instead of ${}^4T_{1g}({}^4G)$, ${}^4T_{1g}({}^4P)$, ${}^4T_{1g}({}^4F)$ and ${}^4T_{2g}({}^4F)$, respectively.

In the present treatment we have not taken into account the width of the observed lines in our calculations which are expected to change our numerical values of V_i 's slightly and bring about better agreement with the lines not involved in the inverse eigenvalues problem. Also, we have appropriately assumed that the possible departures from the cubic symmetry and the spin-orbit interactions in these systems are negligible. Though the theory requires many experimental lines, it is important since it gives information about the various Coulomb and exchange integrals. The present treatment is, however, approximate in the sense that only a restricted manifold of configurations have been incorporated.

The departure from the cubic symmetry at the impurity site due to the F -center has been analyzed by Sibley *et al.* [10]. They observed the nonuniform shift of the lines by as much as 1000 cm^{-1} on comparing the peak positions for the Mn^{2+} transitions in KMnF_3 and MnF_2 with those of the irradiated doped KMgF_3 and MgF_2 . While the observed shifts could be due to the effect of the F -centers, they are partly due to the differences in the crystal structure parameters of the systems analyzed. In view of this one may infer that though some effects on the numerical values of the presently deduced Coulomb and exchange integrals due to the presence of F -centers are expected, it may not be very drastic in changing our present results.

It is hoped that this work will stimulate experiments to observe abundant and sharp lines also in many more crystals with different transition metal ions; it will then be possible to obtain information as to the Coulomb and exchange interactions (together with refined values of Δ) in those systems following the procedure adopted here. Next step in line is to develop the first-principle theory to explain these interaction constants. For this purpose, the theoretical approaches [11] which treat the impurities in solids

appropriately would be very helpful. This, in turn will assist in elucidating the electronic structure of impurities in solids.

In summary, we have used a refined analysis of the transition metal ions in solids which not only reveals the important differences from the conventional three-parameter theory as regards the assignments of the optical lines but also provides estimates of the Coulomb and exchange integrals (along with the refined value of Δ or $10Dq$). This is of great significance since such an information, to the knowledge of the authors, has not been available from any other source. Also, since the present treatment is based entirely on the group theory in conjunction with the experimental data it is expected to give correct assignments to the experimental spectral lines.

Acknowledgement — This work is supported by the United States Office of Naval Research under Contract No. N0001478CO732.

REFERENCES

1. J. Ferguson, *Progress in Inorganic Chemistry* (Edited by S.J. Lippard), Vol. 12, p. 159. Interscience, New York (1970); see also the references cited therein.
2. R. Finkelstein & J.H. Van Vleck, *J. Chem. Phys.* **8**, 790 (1940).
3. Y. Tanabe & S. Sugano, *J. Phys. Soc. Japan* **9**, 753 (1954).
4. J.S. Griffith, *The Theory of Transition Metal Ions*, Cambridge (1961).
5. S.I. Yun, L.A. Kappers & W.A. Sibley, *Phys. Rev.* **B8**, 773 (1973); see also the references cited therein.
6. There are, in fact, three parameters A , B and C but A does not play any role since it gets cancelled in considering energy differences in a given configuration d^n .
7. A. Bohte, *The Computer Journal* **10**, 385 (1968).
8. E. Clementi, *IBM J. Res. Develop.* **9**, 2 (1965).
9. There appears to be a typographical error in the designation of the second line in Table IV of [5] which should read ${}^4T_{2g}({}^4G)$ instead of ${}^4T_{1g}({}^4G)$. Our designation for this line then agrees with that of [5].
10. W.A. Sibley, S.I. Yun & L.N. Fluerheim, *J. de Phys.* **34**, C9-503 (1973).
11. R.R. Sharma & A.M. Stoneham, *Faraday Trans.* II **72**, 913 (1976); J. Callaway, *J. Math. Phys.* **5**, 783 (1964); W. Khon & L.J. Sham, *Phys. Rev.* **A140**, 1133 (1965); O. Gunnarsson & B.I. Lundquist, *Phys. Rev.* **B13**, 4274 (1976); J.C. Slater & K.H. Johnson, *Phys. Rev.* **B5**, 844 (1972); for manybody approach to π -electrons see K.F. Freed, *Theoretical Basis for Semiempirical Theories in Semiempirical Methods of Electronic Structure Calculations* (Edited by I.G. Segal), Vol. I, Plenum Press, New York (1977). See also B.H. Brandow, Formal Theory of Effective π -electron Hamiltonians, *Int. J. Quant. Chem.* **XV**, 207 (1979).

able to derive, from straightforward but tedious group theoretical considerations, the general formula which relates a diagonal element of one with the corresponding one of the other, as

$$\begin{aligned} & \langle t_2^{6-m}(S_1\Gamma_1)e^{4-n}(S_2\Gamma_2)S\Gamma M_s M_{\Gamma} | \cdot | t_2^{6-m}(S_1\Gamma_1)e^{4-n} \\ & \quad \times (S_2\Gamma_2)S\Gamma M_s M_{\Gamma} \rangle - \langle t_2^m(S_1\Gamma_1)e^n(S_2\Gamma_2)S\Gamma M_s M_{\Gamma} | \cdot \\ & \quad \cdot | t_2^m(S_1\Gamma_1)e^n(S_2\Gamma_2)S\Gamma M_s M_{\Gamma} \rangle = (3-m)V_1 + \\ & \quad + 4(3-m)V_2 + (24-4m-6m)\left(\frac{1}{\sqrt{3}}V_3 + V_4\right) + \\ & \quad + (6-3n)V_5 + (5n-10)V_6 + (2m+3n-12)V_7 + \\ & \quad + (2m+3n-12)\frac{1}{\sqrt{3}}V_8 - 2(3-m)V_{10} \end{aligned} \quad (1)$$

where Γ 's are the irreducible representations of the cubic group and S 's are total spin quantum numbers. The importance of this formula arises from the fact that all diagonal elements of a complementary configuration d^{10-n} relative to the configuration d^n are no more altered by the same amount, as it is in case of the simplified theory assuming "pure" d -orbitals and using the Racah parameters.

Knowing the electrostatic matrices we now encounter the problem of determining V_i 's. If sufficient number of experimental lines are available, it is possible, though cumbersome, to determine the V_i 's by solving the relevant inverse eigenvalue problem. By analysis one recognizes that in the free-ion limit, the parameters V_1 , V_2 , V_4 and V_5 contain the Slater-Condon factor F^0 (or the Racah parameter A). Thus, it would be appropriate to use one of the four parameters (as F_0 or A in the free-ion case) to fix the energy scale to facilitate comparison with the spectral lines.

Next, we turn our attention to the interpretation of the optical absorption lines as observed in $MgF_2:Co^{2+}$ and $MgF_2:Mn^{2+}$ by Yun *et al.* [5]. For the related research works one may consult also the review article by Ferguson [1]. In case of $MgF_2:Co^{2+}$ the spin-allowed bands are those of ${}^4A_{2g}$, ${}^4T_{2g}$ and ${}^4T_{1g}^b$ states and the other transitions are spin-forbidden. The spin-forbidden transitions have been observed, as mentioned earlier, by lifting the forbiddenness through exchange interaction with the color-centers. The observed energy values and their tentative assignments based on the previous simplified theory (which effectively assumes "pure" d -type orbitals) have been tabulated in Table 1.

In case of $MgF_2:Co^{2+}$ there are eleven well-defined observed lines (including ${}^4T_{1g}({}^4F)$ as the ground state) out of which ten lines are used for the solution of the inverse eigenvalue problem for determining the ten parameters V_2 , V_3 ... V_{10} , Δ (with V_1

being fixed to identify the ground level with the zero energy); the remaining line can be used for checking the validity of the treatment. For the inverse eigenvalue problem we have derived the d^7 -electrostatic matrices (appropriate to Co^{2+}) containing the unknown parameters V_i . Denoting the electrostatic matrix by M and the energy values by E , one writes,

$$MX = EX$$

where X stands for the eigenfunctions. For the inverse eigenvalue problem one prescribes as many number of eigenvalues as the number of unknown parameters and solves for the parameters, obtaining in the process also the remaining eigenvalues. The dimension N of the matrix varies with the occupancy of the d -orbitals; N is 20 for Co^{2+} which is a d^7 system and it is 43 for $Mn^{2+}(d^5)$. The present inverse eigenvalue problem is indeed very difficult to solve since the number of eigenvalues prescribed is less than the dimension of the matrix. However, we have succeeded in generalizing the method given by Bohte [7] to solve the problem in our case.

The solution of the inverse eigenvalue problem yields the unknown parameters which have been listed in Table 2 for $MgF_2:Co^{2+}$. The calculated energy eigenvalues and the assignments have been given in Table 1 and compared with the observed values and the previous tentative assignments of Yun *et al.* [5] based on the "pure" d -orbital theory. The perusal of Table 1 reveals the important differences that the previous assignments ${}^2T_{1g}({}^2G)$, ${}^2A_{1g}({}^2G)$ and ${}^2T_{1g}({}^2H)$ should respectively be ${}^2T_{2g}({}^2G)$, ${}^2T_{2g}({}^2G)$ and ${}^2A_{1g}({}^2G)$. Also the first ten energy values agree with the observed values as expected and the remaining energy value (${}^2E_g({}^2H)$) lies very close to the observed value. Here we need to emphasize that the present procedure concerns with solving the inverse eigenvalue problem which is basically different from the procedure of fitting with the parameters usually adopted in this field. In Table 2 the Coulomb and exchange integrals calculated for the free- Co^{2+} ion using Clementi's SCF-HF wavefunctions [8] have also been listed for comparison. We have used V_1 for fixing the lowest state at zero energy and, consequently, V_2 , V_4 and V_5 have been shown in Table 2 with respect to V_1 . The calculated value of V_1 for the free-ion case is $217,375 \text{ cm}^{-1}$. It is interesting to note that the derived values of the integrals have changed as much as 50% from the free-ion values. For further comparison the values of the Coulomb and exchange integrals V_i 's are not available from any other source. However, the value of Dq equal to -785 cm^{-1} has been reported for Co^{2+} in fluorine environment (in $KCoF_3$) which lies close to our value of -725 cm^{-1} (Table 2).

As for $MgF_2:Mn^{2+}$ we have used our d^5 -electrostatic

Table 1. Tabulation of the observed [5] and calculated energy values (by solving the inverse-eigenvalue problem as described in the text) for $MgF_2:Co^{2+}$. The previous tentative group theoretical assignments of the levels have also been listed along with the present assignments.

Previous tentative assignments	Observed energy values ^a (cm^{-1})	Calculated energy values ^a (cm^{-1})	Present assignments
$^4T_{2g}(^4F)$	7,519	7,518.9	$^4T_{2g}(^4F)$
$^2E_g(^2G)$	11,905	11,904.9	$^2E_g(^2G)$
	15,385	12,205.1	$^2T_{1g}(^2G)$
$^4A_{2g}(^4F)$	17,452	15,385.0	$^4A_{2g}(^4F)$
$^2T_{1g}(^2G)$	18,519	17,452.1	$^2T_{2g}(^2G)$
$^4T_{1g}(^4P)$	19,305	19,305.0	$^4T_{1g}(^4P)$
	20,921		
$^2A_{1g}(^2G)$	20,833	20,832.9	$^2T_{1g}(^2G)$
$^2T_{1g}(^2H)$	21,739	21,739.0	$^2A_{1g}(^2G)$
$^2T_{2g}, ^2T_{1g}(^2H)$	23,095	23,094.9	$^2T_{2g}(^2H)$
	23,529	23,529.0	$^2T_{1g}(^2H)$
$^2E_g(^2H)$	25,000	26,968.9	$^2E_g(^2H)$

^a With respect to $^4T_{1g}(^4F)$ as the lowest level.

Table 2. List of the Coulomb and exchange interaction constants for Co^{2+} in MgF_2 obtained by the procedure described in the text. The corresponding values calculated by using free-ion SCF-HF wavefunctions have also been given for comparison

Coulomb exchange and crystal field parameters	$V_1 - V_2$	$V_1 - V_4$	$V_1 - V_5$	V_3	V_6	V_7	V_8	V_9	V_{10}	Dq
Present values ^a (cm^{-1})	13,034	13,728	- 2433	2725	8491	3219	1928	1259	6257	- 725
Free ion values ^b (cm^{-1})	16,920	16,920	0	4379	9724	5932	2189	2189	8460	-

^a From the solution of the inverse-eigenvalue problem as explained in the text.

^b Using Clementi's wavefunctions [8]; the calculated value of V_1 for free- Co^{2+} comes out to be $217,375 \text{ cm}^{-1}$.

therefore, the derived electrostatic matrix elements contain 10 independent Coulomb and exchange integrals [4] instead of the three Coulomb repulsion parameters (A , B , and C). The ten independent parameters are: $\langle \xi\xi | \cdot | \xi\xi \rangle$, $\langle \xi\eta | \cdot | \xi\eta \rangle$, $\langle \theta\xi | \cdot | \epsilon\xi \rangle$, $\langle \epsilon\xi | \cdot | \epsilon\xi \rangle$, $\langle \theta\theta | \cdot | \theta\theta \rangle$, $\langle \theta\theta | \cdot | \epsilon\epsilon \rangle$, $\langle \theta\theta | \cdot | \eta\eta \rangle$, $\langle \theta\epsilon | \cdot | \eta\eta \rangle$, $\langle \theta\eta | \cdot | \xi\xi \rangle$ and $\langle \xi\xi | \cdot | \eta\eta \rangle$ which will be referred to as V_1 , V_2 ... and V_{10} , respectively. The V_i 's are the two-electron matrix elements with the "dot" representing the interaction operator e^2/r_{12} , r_{12} being the distance between the two-electrons. The θ , ϵ , ξ , η and ζ stand for the one-electron orbitals in the cubic field

representation. They are not the "pure" d -orbitals if the transition metal ions concerned are embedded in solids since the solid state effects perturb the free-ion d -orbitals. Remaining two-electron integrals which involve θ , ϵ , ξ , η and ζ functions can be shown, from the group theoretical arguments, to be related to the V_i 's.

Since the electrostatic matrix elements are large in number and contain many terms, we do not intend to list them here in terms of the V_i 's. The nondiagonal matrix elements of the complementary states $t_2^{5-m}e^n$ come out to be the same as of the states $t_2^m e^n$. However, the diagonal elements are different. We have been

TRANSITION METAL IONS IN CRYSTALS: A REFINED TREATMENT AND DEDUCTION OF COULOMB AND EXCHANGE INTERACTION CONSTANTS

R.R. Sharma and S. Sundaram

Department of Physics, University of Illinois, Chicago, IL 60680, U.S.A.

(Received 31 July 1979 by G. Burns)

Making use of Racah's irreducible tensor operator technique a refined treatment for the 3d-transition metal ions in crystals has been presented. The refined theory has been applied to analyse the recently observed fine optical spectra of $\text{MgF}_2:\text{Co}^{2+}$ and $\text{MgF}_2:\text{Mn}^{2+}$. Important differences have been noticed in the assignments of the optical lines obtained from the present analysis and from the conventional three-parameter theory. First numerical values of the exchange and Coulomb integrals in these systems have also been given.

THE ELECTRONIC ABSORPTION SPECTRA of the transition metal ions in crystals have been the subject of extensive experimental and theoretical studies [1]. The first application of the theory developed for complex ions in crystals incorporating effects of the electrostatic field of the environment on the free-ion energy levels, was made by Finkelstein and Van Vleck [2] in 1940. Since then many researchers [1, 3-5] have extended our knowledge of the electronic structure of the transition metal ions in solids considerably.

The interpretation of the experimental spectra for the iron-group ions in crystals has hitherto been confined to the use of the Kacah's Coulomb repulsion parameters [6] B and C and the crystal field splitting parameter Δ . The parameters [6] B and C were originally involved in the theory developed by Racah to explain the spectra of free-ions, in particular, the free-iron-group ions. Later on, the theory was extended to explain the optical spectra of the transition metal ions in solids incorporating the effects of the electrostatic crystal fields on the ions assuming that the outermost unfilled electrons were "purely" of d -character, specially in their angular behavior, as in the case of free-ions. Though this assumption simplifies the theory considerably and makes the interpretation very convenient, it is basically faulty since the wavefunctions of an ion undergo changes when it is embedded in a crystal. The inaccuracy of the theory is also revealed by the fact that it does not work well particularly when more spectral lines are involved in the interpretation [2]. Also, in these circumstances, not only that the fitting parameters which it yields are rough in estimates but they (particularly B and C) lose their real physical significance. Moreover, the poor agreement of the calculated energies with the observed spectral lines casts doubts on the correctness of the assignments of the lines predicted by the theory.

In spite of that, the B , C , Δ -theory has served useful purpose owing to the following two main reasons. First, the experimental data were usually scanty with the result that a simple theory involving only a few parameters was good enough to analyse the spectra. Second, no refined theoretical expressions were available for better interpretation even when many spectral lines were provided by the experiments. Recently, Sibley and co-workers [5] and others have performed excellent experiments in which they have been able to observe many sharp lines of the transition metal ions in crystals by lifting the spin-forbiddenness of the excitations through exchange interactions with color centers. These experiments have furnished not only the spin-quartet states but also many hitherto unknown spin-doublets. From these results we have been encouraged to promptly refine the method and use it to analyse the experiments. In the following we first outline the method briefly and apply it to $\text{MgF}_2:\text{Co}^{2+}$ and $\text{MgF}_2:\text{Mn}^{2+}$ where abundant experimental data [5] have recently been obtained.

The present theoretical treatment is well-known and is based on the strong field scheme since the ions of the first transition series in many of their compounds belong to this scheme. The one-electron orbitals are now sets of orbitals which form bases for irreducible representations of the symmetry group of the crystal potential.

The matrices of the electrostatic interaction between the electrons have been determined by utilizing Racah's irreducible tensor operator formalism. This method is not new and has been used previously by Tanabe and Sugano [3] for deriving the electrostatic matrix elements in terms of the Racah parameters A , B and C with the simplifying assumption that the angular parts of the one-electron orbitals are of "pure" d -type. The present derivation is not subjected to this restriction;